STEM CELLS®

TISSUE-SPECIFIC STEM CELLS

Cyclin D3 Critically Regulates the Balance Between Self-Renewal and Differentiation in Skeletal Muscle Stem Cells

GIULIA DE LUCA, ROBERTA FERRETTI, MARCO BRUSCHI, ELEONORA MEZZAROMA, MAURIZIA CARUSO

National Research Council, Institute of Cell Biology and Neurobiology, Fondazione Santa Lucia, Roma, Italy

Key Words. Muscle stem cell • Cell cycle • Self-renewal • Myogenesis • Regeneration • Satellite cell

ABSTRACT

Satellite cells are mitotically quiescent myogenic stem cells resident beneath the basal lamina surrounding adult muscle myofibers. In response to injury, multiple extrinsic signals drive the entry of satellite cells into the cell cycle and then to proliferation, differentiation, and self-renewal of their downstream progeny. Because satellite cells must endure for a lifetime, their cell cycle activity must be carefully controlled to coordinate proliferative expansion and self-renewal with the onset of the differentiation program. In this study, we find that cyclin D3, a member of the family of mitogen-activated D-type cyclins, is critically required for proper developmental progression of myogenic progenitors. Using a cyclin D3-knockout mouse we determined that cyclin D3 deficiency leads to reduced myofiber size and impaired establishment of the satellite cell population within the adult muscle. Cyclin D3-null myogenic progenitors, studied ex vivo on isolated myofibers and in vitro, displayed impaired cell cycle progression, increased differentiation potential, and reduced self-renewal capability. Similarly, silencing of cyclin D3 in C2 myoblasts caused anticipated exit from the cell cycle and precocious onset of terminal differentiation. After induced muscle damage, cyclin D3-null myogenic progenitors exhibited proliferation deficits, a precocious ability to form newly generated myofibers and a reduced capability to repopulate the satellite cell niche at later stages of the regeneration process. These results indicate that cyclin D3 plays a cell-autonomous and nonredundant function in regulating the dynamic balance between proliferation, differentiation, and self-renewal that normally establishes an appropriate pool size of adult satellite cells. STEM CELLS *2013;31:2478–2491*

Disclosure of potential conflicts of interest is found at the end of this article.

INTRODUCTION

Growth and repair of skeletal muscle rely on tissue-specific stem cells, termed satellite cells. In adult muscle, satellite cells are associated with myofibers and are quiescent, but in response to muscle injury they become activated, express the muscle regulatory factor MyoD, and enter the cell cycle. The majority of myogenic progenitor cells then differentiate to repair damaged myofibers, whereas a small proportion downregulates MyoD and returns to quiescence by both symmetric and asymmetric divisions to replenish the satellite cell compartment [1–5]. Targeted gene knockout has revealed that the absence of MyoD delays the early proliferation response of activated satellite cells and affects the differentiation potential of myogenic precursors, thus impairing muscle regeneration [6–10]. MyoD is, therefore, implicated in both the proliferation and differentiation phases of progression of the satellite cell lineage, whereas MyoD suppression in quiescent satellite cells seems to be essential for maintaining the undifferentiated state.

MyoD couples the onset of differentiation with cell-cycle arrest by inducing the myogenic regulatory factor myogenin and a number of cell-cycle inhibitors, including the retinoblastoma protein (pRb) and the cyclin-dependent-kinase inhibitors (CKIs) p21 and p57 [11–14]. Furthermore, MyoD contributes to cell-cycle withdrawal by downregulating the activity of NF-kB, possibly through induction of the PC4 protein [15,16]. However, MyoD also appears to induce the expression of factors deputed to promote cell division, such as cyclin D3 and the DNA replication licensing factor cdc6 [17–19].

D-type cyclins (D1, D2, and D3) are components of the core cell cycle machinery whose expression is induced by extracellular mitogenic stimulation during the early G1 phase [20]. A common function of D-type cyclins is to initiate phosphorylation of pRb in association with partner cyclin-dependent kinases CDK4 and CDK6. This leads to derepression of E2F transcription factors, activation of cyclin E, and progression of the cells into the mitogen-independent late G1 phase [21,22].

D-cyclins are highly homologous suggesting redundancy in their functions. However, there is much evidence that they also differ in many ways, such as the tissue-specific expression pattern and different induction by various signals in a cell lineage-specific manner; there are different phenotypic consequences of cyclin D knockouts in mice, and they impart distinct site-specificities for pRb phosphorylation to their

Author contributions: G.D.L., R.F., M.B., and E.M.: collection and assembly of data and data analysis and interpretation; M.C.: conception and design, data analysis and interpretation, manuscript writing, and financial support. G.D.L. and R.F. contributed equally to this article.

Correspondence: Maurizia Caruso, Ph.D., National Research Council, Institute of Cell Biology and Neurobiology, Fondazione Santa Lucia, Via del Fosso di Fiorano, 64, 00143 Roma, Italy. Telephone: 39-06501703186; Fax: 39-06501703311; e-mail: maurizia.caruso@cnr.it Received March 7, 2013; accepted for publication June 21, 2013; first published online in STEM CELLS *EXPRESS* July 29, 2013. 1066-5099/2013/$30.00/0 doi: 10.1002/stem.1487

kinase partners [23–29]. Furthermore, there is considerable evidence that D-type cyclins may also perform cell cycle-independent, nonredundant functions as transcription coregulators [30–35].

Asynchronously proliferating C2 myoblasts express variable levels of the three D-type cyclins. When they are induced to differentiate in low-mitogen medium, expression of cyclin D1 and D2 rapidly declines, whereas that of cyclin D3 is induced at the transcriptional and post-translational level through MyoD- and pRb-mediated mechanisms [15,17,18,36–39]. The distinct expression patterns of D-type cyclins suggest that cyclin D3 may perform a unique function during myogenesis. This notion is further supported by the observations that overexpression of cyclin D1, but not D3, inhibits MyoD function and myogenic differentiation [37,38,40,41]. Indeed, ectopic expression of a stabilized cyclin D3 delays pRb dephosphorylation and irreversible exit from the cell cycle, but is fully compatible with terminal differentiation of C2 myoblasts [39].

In skeletal muscle, cyclin D3 is expressed at high levels during the late stages of fetal development and early postnatal life [42], when satellite cells contribute progeny that fuse to the enlarging myofibers. Also, expression of cyclin D3 mRNA is increased in mdx muscle that has successfully regenerated [43]. These observations argue for a function of cyclin D3 in the establishment of muscle cell differentiation and suggest a role for cyclin D3 during satellite cell-mediated postnatal muscle growth and adult regenerative myogenesis. In this study, we have investigated the role of cyclin D3 in myogenesis using RNA-interference to knockdown cyclin D3 in cultured myoblasts and a cyclin D3-null mouse model to analyze the effects of cyclin D3 loss on satellite cell behavior in vivo and ex vivo. We find that cyclin D3 plays a nonredundant function in regulating the dynamic balance between proliferation, differentiation, and self-renewal that normally establishes an appropriate pool size of adult satellite cells.

Materials and Methods

Mice

Cyclin $D3^{-/-}$ mice were provided by Piotr Sicinski. Wild-type (WT) controls were generated along with $D3^{-/-}$ mice by interbreeding heterozygous animals. Mice were genotyped as previously described [26]. For all experiments, we used 2–3-month-old cyclin $D3^{-/-}$ and WT littermates.

Mice were anesthetized by intraperitoneal administration of chloralium hydrate (0.45 mg/g b.wt.) and the tibialis anterior (TA) muscle was injected with 20 μl of a 10^{-5} M solution of cardiotoxin in NaCl 0.9% (Latoxan, Valence, France, www.latoxan.com). For detection of satellite cell proliferation, 10 μl/mouse gram of a 9.6 mg/ml solution of 5-bromo-2'-deoxyuridine (BrdU, Sigma-Aldrich, St. Louis, MO, www.sigmaaldrich.com) in Phosphate Buffered Saline (PBS) was injected intraperitoneally 6 hours before sacrifice. All animal procedures were completed in accordance with the current European (directive 2010/63/EU) Ethical Committee guidelines.

Cell Lines and Transfections

C2.7 mouse myoblasts (a subclone of C2 myoblasts, [44]) were cultured in Dulbecco's modified Eagle's medium (DMEM, Invitrogen/Gibco, Carlsbad CA, www.invitrogen.com) supplemented with 20% fetal bovine serum (FBS, HyClone Laboratories, South Logan, UT, www.thermo.com/hyclone). Differentiation was induced by exposing myoblast cultures to DMEM containing 2% horse serum (HyClone). The Phoenix ecotropic packaging cell line was cultured in DMEM supplemented with 10% FBS. DNA transfections were carried out with Lipofectamine (Invitrogen) according to the manufacturer's instruction.

Retroviral Constructs, Production of Retroviruses, and Retroviral Infections

Constructs expressing shRNA directed against cyclin D3 were prepared in the Murine Stem Cell Virus-based pLMP retroviral vector (OpenBiosystems, Thermo Scientific, Waltham, MA, www.thermoscientificbio.com/openbiosystems/) following described procedures [45,46]. The hairpin used in the study is as follows: CTGGCCCTCTGTGCTACAGATT. Retroviral constructs were transfected into Phoenix-ECO packaging cells; retrovirus-containing supernatants were collected at 48 and 72 hours after transfection and immediately used to infect C2.7 cells for 2 consecutive days (one infection per day) for 7 hours. Infected cells were then selected for 3 days with 2 μg/ml of Puromycin (Sigma-Aldrich), and the resulting puromycin-resistant cell populations reseeded for the corresponding assays (carried out at days 5–9).

Primary Myoblast Preparation

Hind limb muscles were dissected and incubated with 0.2% collagenase type-I (Sigma-Aldrich) in DMEM for 30 minutes at 37°C, followed by a second digest in 2 mg/ml Collagenase/Dispase (Roche Diagnostics GmbH Mannheim, Germany, www.roche.com) for 30 minutes at 37°C. Satellite cells were mechanically dissociated by passing the tissue suspension through a 5 ml pipette; the slurry was sequentially filtered through 70 and 40 μm cell strainers (BD Biosciences, Bedford, MA, www.bdbiosciences.com) and centrifuged. Pelleted cells were resuspended in F-10 (Invitrogen/GIBCO) supplemented with 20% FBS and 2.5 ng/ml basic-fibroblast growth factor (Peprotech, Rochy Hill NJ, www.peprotech.com). The cell suspension was preplated for 1 hour on uncoated dishes to remove fibroblasts. The medium containing the enriched myoblast population was then plated on tissue culture dishes coated with type-I collagen (Sigma-Aldrich).

Single Fiber Preparation

Extensor digitorum longus (EDL) muscles were digested using 0.2% collagenase type-II (Sigma) in DMEM for 60–70 minutes at 37°C with shaking. Muscles were mechanically dissociated and single fibers liberated. After extensive washing, myofibers were either immediately fixed or cultured in plating medium (DMEM supplemented with 10% horse serum and 0.5% chick embryo extract [USBiological, Swampscott, MA, www.usbio.net]) in suspension.

For satellite cell cultures, single myofibers were plated on 24-well dishes coated with Matrigel (BD-Biosciences, 1 mg/ml in DMEM) in plating medium. After 2 days, fibers were removed and the medium replaced with proliferation medium (DMEM, 20% FBS, 10% horse serum, and 1% chick embryo extract).

Immunofluorescence

For cryostat sections, TA muscles were embedded in Tissue-Tek OCT (Sakura Finetek Europe, Zoeterwoude, NL, www.sakuraeu.com) and frozen in liquid nitrogen-cooled isopentane. Nine-micrometer thick cryosections were fixed using 4% Paraformaldehyde (PFA), quenched in 0.1 M glycine, and permeabilized with 0.1% Triton X-100/PBS for 10 minutes.

For Pax7 and MyoD staining, antigen retrieval was done by immersing slides in a solution of 10 mM sodium citrate pH-6 preheated to 90°C in a microwave, and then cooled at room temperature. The slides were rinsed in PBS and blocked for 2 hours in 4% Bovine Serum Albumin/PBS or in 3% goat serum/PBS. Slides were further incubated with goat anti-mouse AffiPure Fab

fragment (Jackson ImmunoResearch, West Grove, PA, www.jireurope.com) to block endogenous mouse IgG.

For detection of labeled DNA, samples were postfixed with 4% PFA after primary and secondary staining, denatured in 2 M HCl for 20 minutes, and neutralized by washing twice with Na Borate pH 8. Samples were then permeabilized/blocked for 1 hour in 0.1% Triton X-100, 0.03% Tween/PBS plus 3% donkey serum.

For processing cells for immunofluorescence, primary myoblasts were cultured on eight-well Lab-tek chamber slides (Nalge Nunc International Rochester, New York, www.nuncbrand.com) coated with Matrigel. Cells were fixed in 4% PFA, quenched with glycine 50 mM, permeabilized with 0.5% Triton X-100/PBS for 10 minutes, and then blocked in PBS containing 10% donkey and/or goat serum for 1 hour. Single fibers in suspension were fixed in 2% PFA for 10 minutes, quenched in glycine 100 mM, permeabilized with 0.5% Triton X-100/PBS, and blocked with 20% goat serum/PBS for 1 hour.

Primary antibodies were applied overnight at 4°C, and fluorophore-conjugated, species-specific secondary antibodies were applied 1 hour at room temperature. Samples were then washed with PBS and cellular DNA was labeled with 4′,6-diamidino-2-phenylindole (0.1 μg/ml in PBS). Primary and secondary antibodies used are listed in Supporting Information Table S1.

Western Blot

For preparation of whole-cell extracts, cells were lysed in "Urea buffer" containing 8 M Urea, 100 mM NaH_2PO_4, and 10 mM Tris HCl pH 8. For preparation of muscle tissue extracts, hind limb muscles were homogenized in SDS Lysis buffer (1 ml/100 mg of tissue weight). Western blot analysis was performed using the primary and horseradish peroxidase-conjugated secondary antibodies (Jackson ImmunoResearch) listed in Supporting Information Table S1.

Quantitative RT-PCR

Total cellular RNA was prepared according to the procedure of Chomczynski and Sacchi [47], and retrotranscribed using Moloney Murine Leukemia Virus reverse transcriptase (Invitrogen). Quantitative real-time PCR (qPCR) was performed using TaqMan probe-based fluorogenic 5′-nuclease chemistry and a 7900HT System (Applied Biosystems, Foster City, CA, www.appliedbiosystems.com). The mRNA expression values were normalized to those of the TATA-binding protein gene. qPCR assays were designed using the ProbeFinder software (Universal Probe Library system, Roche, www.roche-applied-science.com). Gene-specific primer sets and probes are listed in Supporting Information Table S2.

Statistical Analysis

For all quantitative analyses presented, a minimum of three replicates were performed in terms of independent experiments or individual mice. For quantification from cryosections, at least three sections per mouse were analyzed. Two-tailed Student's *t* test was used to calculate *p* values and determine statistically significant differences.

Results

Genetic Knockdown of Cyclin D3 in Myoblasts Leads to Impaired Proliferation and Premature Expression of Myogenic Differentiation Genes

To start investigating the role of cyclin D3 in myogenesis, we targeted cyclin D3 by RNA interference in the C2.7 myogenic cell line. Figure 1 shows a time course expression analysis of relevant muscle-specific and cell cycle regulatory factors during differentiation of myoblasts transduced with a retrovirus expressing a cyclin D3-specific short hairpin RNA sequence (shCyclinD3) or the empty retrovirus. The expression of cyclin D3 mRNA, which is normally induced in differentiating myoblasts, was efficiently inhibited by the shCyclinD3 (Fig. 1A). Compared with controls, cyclin D3-depleted myoblasts displayed higher levels of MyoD transcript and premature induction of the myogenin and myosin heavy chain (MHC) differentiation markers. Furthermore, the typical expression pattern of the Pax7 transcription factor was temporally anticipated following cyclin D3 knockdown (Fig. 1A). Altogether, this indicated faster differentiation kinetics for cyclin D3-deprived myoblasts.

Myogenic differentiation entails downregulation of most cyclins and upregulation of cell cycle inhibitors, including retinoblastoma (Rb) and the CKI p21. Cyclin D3 depletion did not alter the expression patterns of cyclin D1 and cyclin A, whereas the Rb and p21 transcripts were induced more rapidly (Fig. 1A). The changes in mRNA expression elicited by cyclin D3 knockdown were accompanied by similar changes in protein levels with the exception of p21 (Fig. 1B, 1C). In fact, cyclin D3-deprived myoblasts accumulated greatly reduced levels of the p21 protein despite induction of p21 transcript, suggesting that cyclin D3 regulates p21 expression post-transcriptionally.

Next, we investigated the effects of cyclin D3 knockdown on myoblast proliferation. Cell cycle profile analyses showed that cyclin D3-depleted myoblast cultures contained a significantly increased percentage of cells in the G0/G1 phase relative to control cells. This was accompanied by a decrease in the S-phase cell population, both in proliferation medium and during the first 24 hours in differentiation medium (Fig. 2A). Accordingly, parallel cell growth curves indicated a reduced proliferative capacity for cyclin D3-depleted myoblasts (Fig. 2B). Cyclin D3 knockdown in C2.7 myoblasts results, therefore, in impaired cell cycle progression and anticipated exit from the cell cycle in low-mitogen medium.

Following terminal differentiation, cyclin D3-deprived myoblasts formed multinucleated myotubes that were reduced in number and size compared with control myotubes, presumably as a consequence of their proliferation deficit (Fig. 2C). Indeed, if cells were plated at high density and immediately shifted to differentiation medium, we could observe again a premature expression of myogenic differentiation genes and downregulation of p21 in cyclin D3-deprived myoblasts, while the efficiency of myotube formation was similar to that of control myoblasts (Supporting Information Fig. S1).

Cyclin D3 Deficient Muscle Displays Smaller Fiber Size and Decreased Number of Satellite Cells

To explore a potential function for cyclin D3 in postnatal myogenesis in vivo, we first examined the expression of cyclin D3 protein in limb muscles harvested from 7- to 60-day-old mice (Fig. 3A). Cyclin D3 was highly expressed during the first 2 weeks of postnatal life along with markers of proliferating and early differentiating muscle progenitors, such as Pax7, cyclin D1, MyoD, and myogenin. All these proteins became undetectable after P21, consistent with cessation of postnatal muscle accretion. Likewise, cyclin D3 and proliferation/differentiation markers resulted highly expressed in 2-month-old (P60) muscle during the early phase of cardiotoxin-induced regeneration, when satellite cells are activated to provide new myonuclei for muscle repair (Fig. 3A).

To determine the function of cyclin D3 in skeletal muscle and satellite cells, we analyzed the adult muscle phenotype of cyclin D3 knockout ($D3^{-/-}$) mice [26]. These mice were

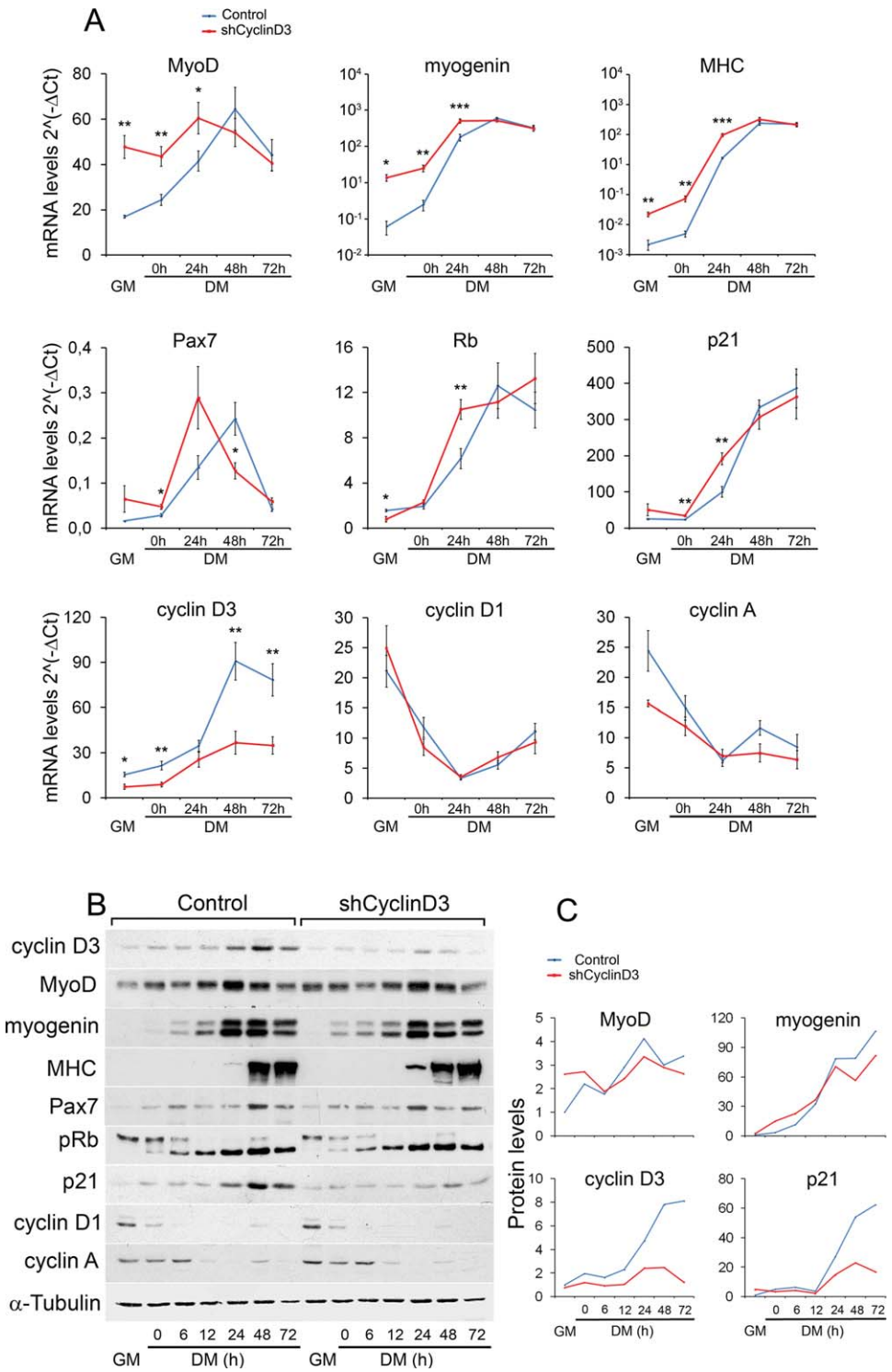

Figure 1. Cyclin D3 knockdown in myoblasts leads to precocious onset of differentiation. C2.7 myoblasts transduced either with the retrovirus expressing cyclin D3-specific shRNA (shCyclin D3) or with the empty retrovirus (control) were seeded at 2×10^5 cells into 90-mm dishes, and transferred to DM after 48 hours. Total RNA and whole-cell extracts were prepared from cells collected in GM 24 hours after seeding or at indicated times after exposure to DM. **(A):** RT-qPCR analysis was performed on the genes indicated. Graphs represent average $2^{-\Delta CT}$ values ± SEM from four independent experiments. **(B):** Western blot analysis was performed using antibodies specific for the indicated proteins. **(C):** Quantification of protein expression by densitometry analysis of Western blots shown in (B); values are presented as fold change relative to control myoblasts cultured in GM (set to 1), after normalization to the corresponding values of α-tubulin levels. Asterisks denote significance (*, $p < .05$; **, $p < .01$; ***, $p < .001$). Abbreviations: DM, differentiation medium; GM, growth medium; MHC, myosin heavy chain; Rb, retinoblastoma gene; pRb, retinoblastoma protein.

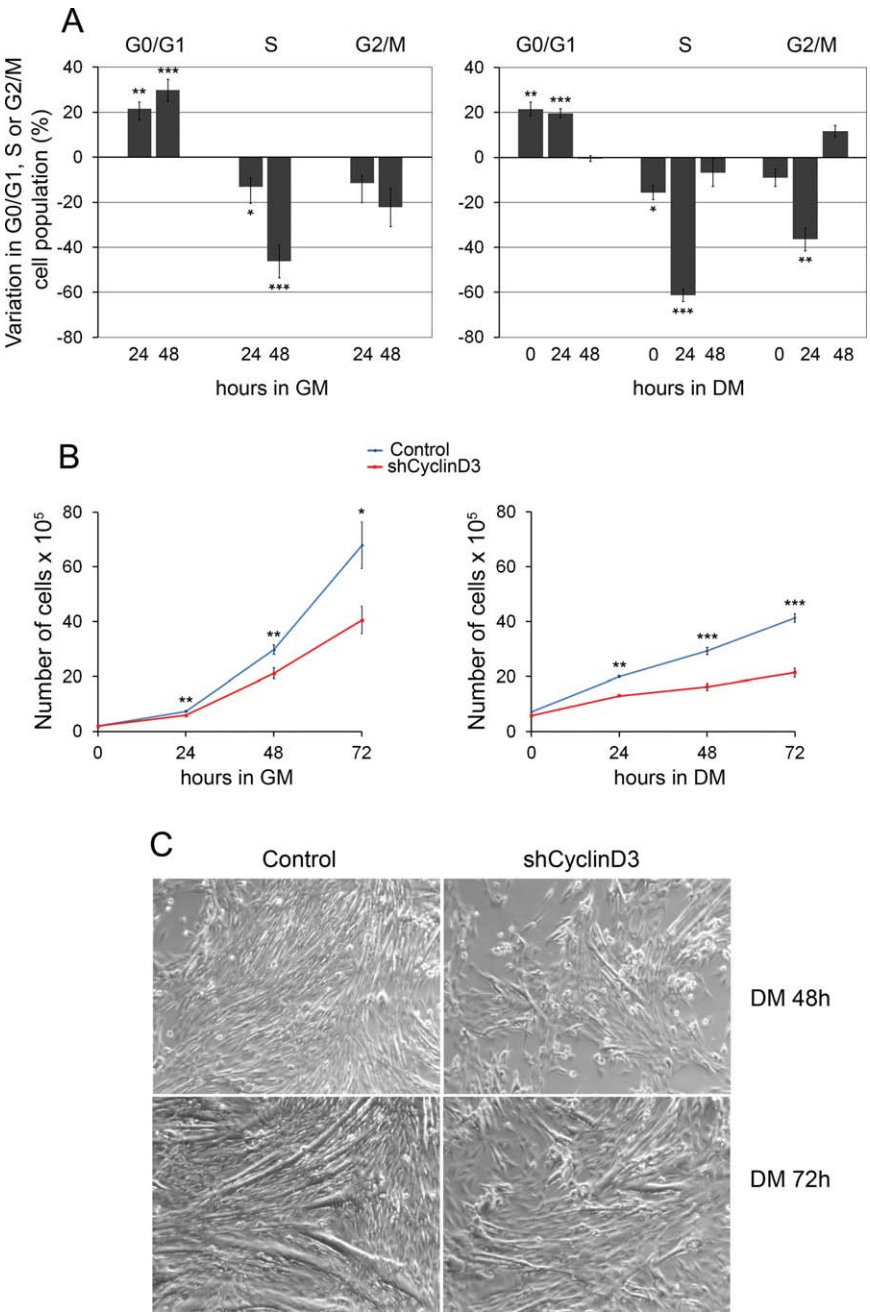

Figure 2. Cyclin D3 knockdown in myoblasts results in reduced proliferation, accelerated exit from the cell cycle, and impaired myotube formation. C2.7 myoblasts transduced either with the retrovirus expressing shCyclinD3 or with the control retrovirus were seeded at 2×10^5 cells into 90-mm dishes and either cultured in GM for 72 hours or transferred to DM 24 hours after seeding. **(A):** Cells cultured in GM (left panel) or in DM (right panel) were harvested at the indicated time points, stained with propidium iodide, and analyzed by flow cytometry. Data are presented as changes in the percentage of shCyclinD3 cells, in particular phases of cell cycle at each time point, relative to control cells. Error bars represent SEM (±SEM) for five independent experiments. **(B):** Cells cultured in GM (left panel) or in DM (right panel) were counted at the indicated time points. Graphs represent average cell numbers ± SEM ($n = 5$). **(C):** shCyclin D3 or control myoblasts were seeded at 2×10^5 cells into 90-mm dishes, and transferred to DM after 48 hours. Phase-contrast microphotographs (whole ×20 field) show cells induced to differentiate for 2–3 days. Asterisks denote significance (*, $p < .05$; **, $p < .01$; ***, $p < .001$). Abbreviations: DM, differentiation medium; GM, growth medium.

similar to WT littermates at birth but showed growth retardation, and when adult, they exhibited significantly decreased body and muscle weight. The loss of muscle weight in $D3^{-/-}$ mice was not merely a consequence of the decreased body weight because we observed also a significant reduction of muscle mass in these animals (Fig. 3B). When the myofiber size and number were quantified in transverse sections of TA muscles collected from P60 mice, we found that cyclin $D3^{-/-}$ myofibers were smaller in size and reduced in number compared with WT myofibers (Fig. 3C, 3D). Then, we examined the satellite cell population of P60 mice. Compared with control mice, the number of Pax7-positive cells contained in TA

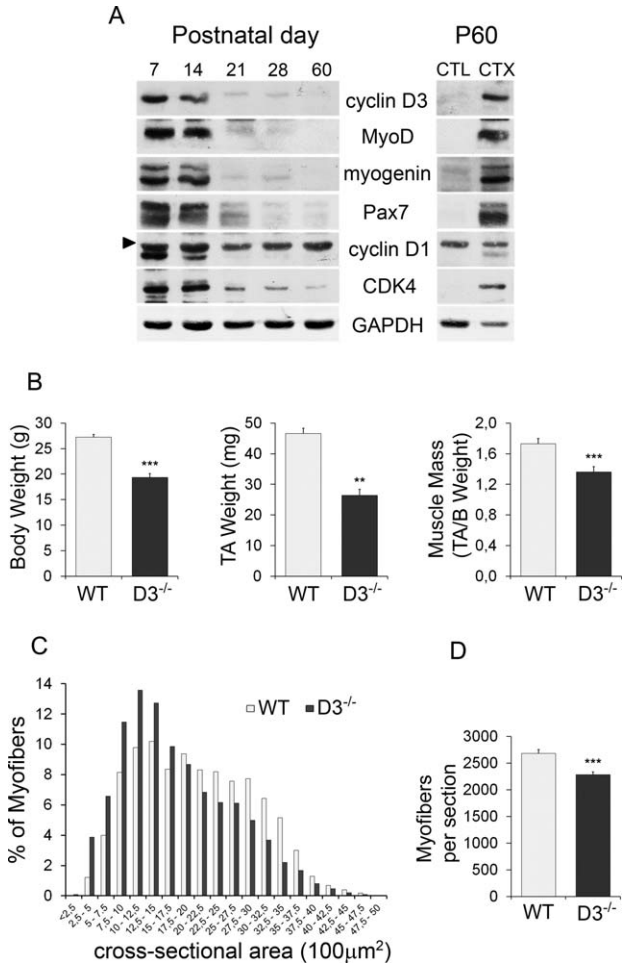

Figure 3. Cyclin D3 deficiency in vivo results in postnatal muscle defects. **(A):** Cyclin D3 is highly expressed in muscle during postnatal and regenerative myogenesis. Western blot analysis of extracts prepared from hind limb muscles of 7–60-day-old mice and from uninjured (CTL) or injured tibialis anterior muscles of 60-day-old (P60) mice. Injury was induced by injection of CTX, and muscle was collected after 3 days. Immunoblots were probed with the indicated antibodies. The arrow head indicates a non-specific band **(B):** Average body weight, TA muscle weight, and TA muscle mass of 70–85-day-old wild-type (WT) and cyclin D3$^{-/-}$ (D3$^{-/-}$) male mice. Error bars represent ±SEM for $n = 6$. **(C):** Frequency histogram showing the myofiber cross-sectional area measured on transversal sections of TA muscles from WT and D3$^{-/-}$ male mice at P60 ($n = 3$; WT: 4,033 myofibers, D3$^{-/-}$: 3,701 myofibers). **(D):** Average number ±SEM of myofibers per TA cryosection in P60 WT and D3$^{-/-}$ male mice ($n = 3$). Asterisks denote significance (**, $p < .01$; ***, $p < .001$). Abbreviations: CTX, cardiotoxin; TA, tibialis anterior; WT, wild type.

cross-sections was reduced by about 30% in D3$^{-/-}$ animals (Fig. 4A, 4B). This finding was complemented and confirmed by the enumeration of Pax7^{+} cells on single myofibers freshly isolated from EDL muscles. We found, indeed, that the mean number of Pax7^{+}cells resident on cyclin-null myofibers was reduced by about 40% when compared with that of WT myofibers (Fig. 4C, 4D). Cyclin D3 deficiency results, therefore, in adult muscle defects characterized by reduced myofiber number and size and reduced number of sublaminar satellite cells, suggesting that cyclin D3 is involved in the establishment of the adult satellite cell pool occurring during postnatal muscle development.

Cyclin D3 Loss Affects Satellite Cell Differentiation and Self-Renewal

The adult muscle defects of cyclin D3-null mice could be due to a dysfunction of satellite cells. To examine the effects of cyclin D3 loss on satellite cell behavior, we analyzed the properties of myofiber-associated satellite cells. Cyclin D3 deficiency did not affect satellite cell activation, since immunofluorescence analysis of single EDL fibers 6 hours ex vivo indicated that by this time, a similar fraction of satellite cells had become activated on both cycD3-null and control myofibers, as shown by the presence of MyoD (Fig. 4E).

After 72 hours in culture, immunostaining of EDL myofibers from cyclin D3-null and control mice showed the typical clusters of satellite cell progeny undergoing proliferation, differentiation, and self-renewal, distinguished as Pax7^{+}/MyoD^{+}, Pax7^{-}/MyoD^{+}, and Pax7^{+}/MyoD^{-}, respectively [48]. Quantification of the number of cells in each category revealed a significant increase of Pax7^{-}/MyoD^{+} cells, and a parallel decrease of Pax7^{+}/MyoD^{-} cells, on cyclin D3-null myofibers compared with WT controls, which indicates a precocious onset of differentiation (Fig. 5A, 5B). Coimmunostaining for Pax7 and myogenin confirmed a significant increase in the fraction of cells with the differentiating phenotype (Pax7^{-}/myogenin^{+}) on cyclin D3-null myofibers, with a reciprocal decrease of self-renewing (Pax7^{+}/myogenin^{-}) cells (Fig. 5C, 5D). Overall, the average number of satellite cell progeny within each cluster of cells growing on cyclin D3$^{-/-}$ myofibers was reduced compared to WT myofibers (Fig. 5E). Therefore, loss of cyclin D3 results in a shift toward differentiation in the self-renewal/differentiation balance.

To examine the effects of cyclin D3 deficiency on the later stages of myogenesis, satellite cells released from EDL myofibers were plated and allowed to differentiate for 3 days. Coimmunostaining for Pax7 and MHC revealed that the differentiation index of cyclinD3-null cells was slightly higher than that of WT cells, and this was accompanied by a substantial decrease in the frequency of Pax7-positive undifferentiated cells (55% of control) (Fig. 5F--5H). These results indicate that cyclinD3-null myogenic progenitors have a higher propensity to fuse into multinucleated myotubes, and a reduced ability to generate undifferentiated "reserve" cells, which represent an in vitro model of in vivo quiescent satellite cells.

Then, we analyzed the expression profile of cyclin D3 in myofiber-associated satellite cells. The expression of cyclin D3 was undetectable in satellite cells 6 hours ex vivo (data not shown), and at low levels after culturing myofibers for 48 hours (Supporting Information Fig. S2A). At 72 hours, coimmunostaining for cyclin D3 and either MyoD, myogenin, or Pax7 showed that cyclin D3 was highly expressed in the vast majority of MyoD^{+} and myogenin^{+} cells but only in a small fraction of Pax7-positive cells (Supporting Information Fig. S2B--S2D). Furthermore, differentiated cultures of plated satellite cells showed strong nuclear staining for cyclin D3 in myotubes but not in mononucleated undifferentiated cells (Supporting Information Fig. S2E). The high expression of cyclin D3 in cells with the differentiating phenotype is in line with our previous studies showing that cyclin D3 protein becomes stabilized upon myogenic differentiation [39].

Cyclin D3 Null Satellite Cells Have a Reduced Capacity to Proliferate In Vitro

To further elucidate the features of cyclin D3-null satellite cells, we analyzed primary myoblasts prepared from hind limb muscles. An equivalent number of cyclin D3-null or control primary myoblasts was plated, and cultured for 24,

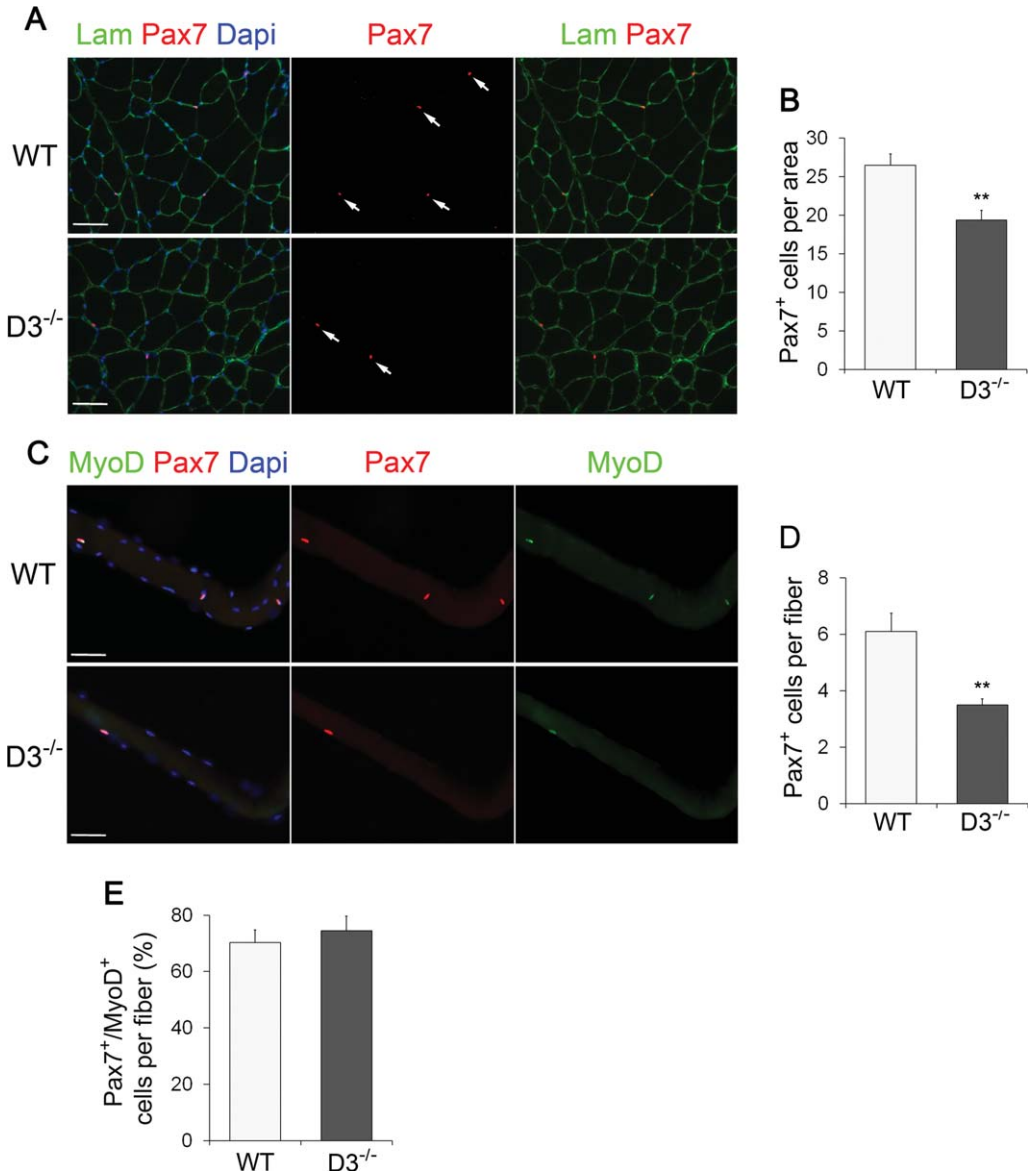

Figure 4. Ablation of cyclin D3 leads to a decline in the adult satellite cell pool size. **(A):** Transverse sections of tibialis anterior muscles from WT and $D3^{-/-}$ male mice at P60 were stained with Laminin to identify myofibers (green) and Pax7 to identify sublaminar satellite cells (red) indicated by arrows. Nuclei were counterstained with Dapi (blue). **(B):** Average number of Pax7-positive cells per cross-sectional tissue area (mm^2) in WT and $D3^{-/-}$ mice. Error bars represent ±SEM for $n = 3$. **(C):** Single myofibers freshly isolated from extensor digitorum longus muscles of 8–12-week-old WT and $D3^{-/-}$ mice were stained 6 hours ex vivo for Pax7 (red) and MyoD (green), and counterstained with Dapi (blue). **(D)**: Average number of $Pax7^+$ satellite cells per myofiber in WT and $D3^{-/-}$ mice. Error bars represent ±SEM for $n = 5$ WT and $n = 7$ $D3^{-/-}$. **(E):** Quantification of $Pax7^+/MyoD^+$ satellite cells per myofiber in WT and $D3^{-/-}$ mice. Values are expressed as the mean percentage of $Pax7^+$ cells that were MyoD-positive (means ± SEM for $n = 4$). Asterisks denote significance (**, $p < .01$). Scale bar = 50 μm. Abbreviations: Lam, Laminin; Dapi, 4′,6-diamidino-2-phenylindole; WT, wild type.

48, and 72 hours, respectively. A significant decrease in the number of cyclin $D3^{-/-}$ cells was observed after 3 days in culture, indicating a reduced proliferative capacity (Fig. 6A). When we compared the cell cycle distribution of cyclin $D3^{-/-}$ myoblasts versus control myoblasts cultured for 48 hours, we found that a significantly lower percentage of $D3^{-/-}$ cells were in S-phase (30% reduction), which was accompanied by an increase in the G0/G1 and G2/M cell populations (Fig. 6B). To further estimate the proliferative potential of cyclin D3-deficient satellite cells, we assessed the percentage of cells in S-phase and mitosis using a 4-hour BrdU pulse label and immunostaining with anti-phospho-Histone H3, respectively. A significant reduction in the frequency of $MyoD^+/BrdU^+$ cells was observed in cyclin $D3^{-/-}$ cultures compared to WT controls (Fig. 6C, 6D). Also, fewer cyclin D3-null than WT myoblasts were found in mitosis (Fig. 6E, 6F).

In agreement with the results obtained with primary myoblasts from bulk muscle, we observed a significant decrease in the fraction of cells in S-phase in cyclin $D3^{-/-}$ satellite cell cultures derived from isolated EDL myofibers (Supporting Information Fig. S3A). Immunostaining for activated caspase-3 did not reveal any evidence of apoptosis in cyclin D3-null cells (Supporting Information Fig. S3B). Together,

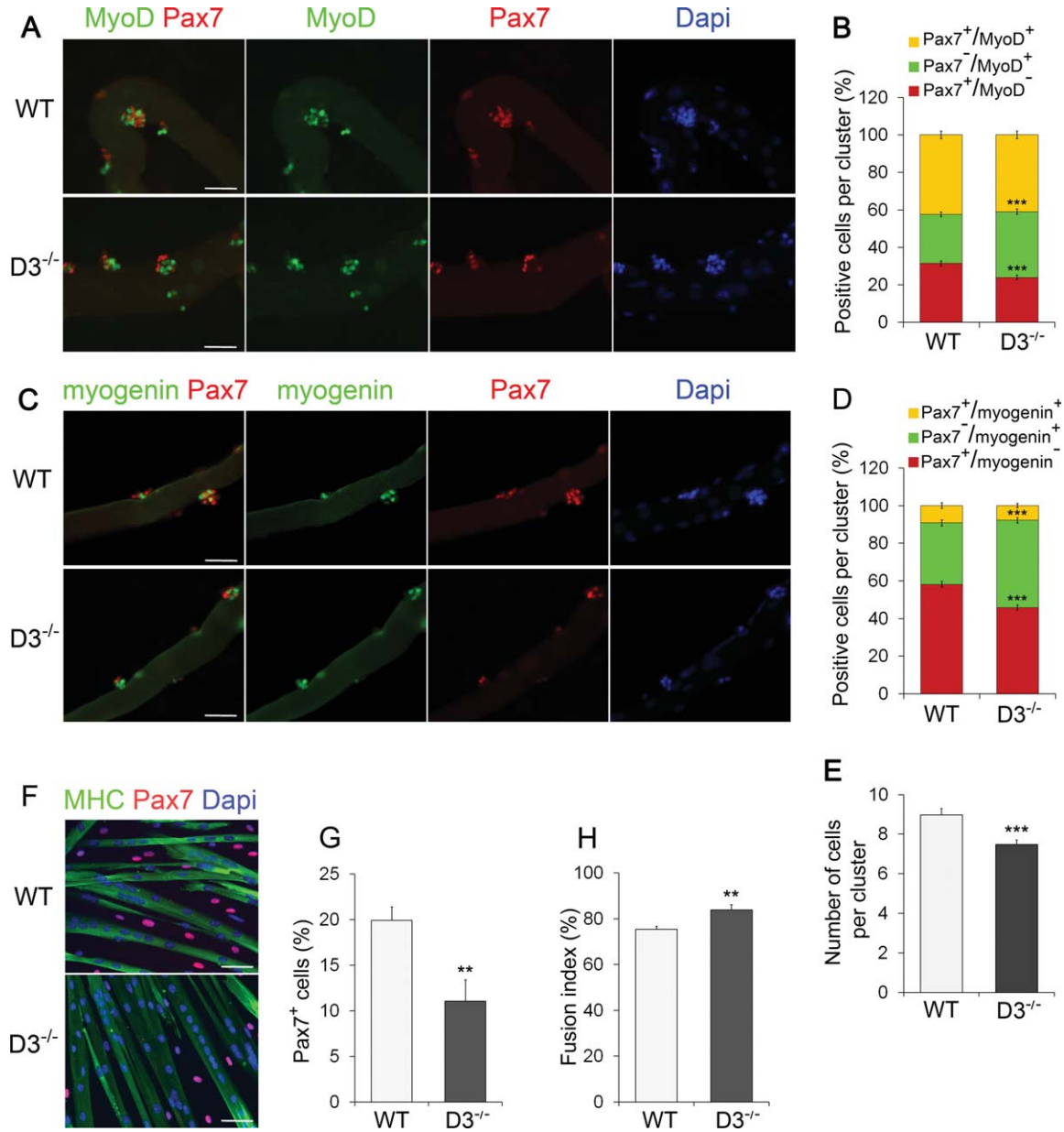

Figure 5. Cyclin D3 loss affects SC differentiation and self-renewal. **(A):** Batches of single extensor digitorum longus (EDL) myofibers from WT and D3$^{-/-}$ mice were coimmunostained for Pax7 (red) and MyoD (green) after 72 hours in suspension culture. Counterstaining with Dapi (blue) was used to identify all nuclei present on the myofiber. **(B):** The graph represents the quantification of the Pax7^{+}/MyoD^{-}, Pax7^{+}/MyoD^{+}, or Pax7^{-}/MyoD^{+} cells contained in clusters of four or more cells. Data are expressed as the percentage in each category of the total positive cells per cluster (means ± SEM). Clusters (270) from WT ($n = 4$) and D3$^{-/-}$ ($n = 3$) mice were analyzed, for a total of 2,000 cells counted for each genotype. **(C):** Myogenin (green) and Pax7 (red) coimmunostaining of WT and D3$^{-/-}$ EDL myofibers 72 hours after isolation, and counterstaining with Dapi (blue). **(D):** The graph represents the quantification of the Pax7^{+}/Myogenin^{-}, Pax7^{+}/Myogenin^{+}, or Pax7^{-}/Myogenin^{+} cells. Data are expressed as in (B). Clusters (180) from WT ($n = 3$) and D3$^{-/-}$ ($n = 5$) mice were analyzed, for a total of 1,300 cells counted for each genotype. **(E):** Quantification of cluster size. The total number of cells present in the WT and D3$^{-/-}$ clusters analyzed in (B) was calculated and expressed as mean number of cells per cluster ± SEM. **(F):** Satellite cells derived from WT and D3$^{-/-}$ EDL myofibers were seeded in eight-well permanox chamber slides (1.2×10^4/well) and transferred to DM after 24 hours. Cells were cultured in differentiation medium for 72 hours before fixing and immunostaining for MHC (green) to visualize myotubes and Pax7 to identify mononuclear undifferentiated reserve cells (red). Counterstaining with Dapi was used to visualize all nuclei (blue). **(G):** Relative number of Pax7-expressing cells. Values are expressed as the mean percentage ± SEM of total nuclei (WT: $n = 6$; D3$^{-/-}$: $n = 5$). **(H):** Quantification of fusion index. Values are expressed as the mean ratio ± SEM of nuclei present in myotubes to the total number of nuclei ($n = 5$). Asterisks denote significance (**, $p < .01$; ***, $p < .001$). Scale bar = 50 μm. Abbreviations: Dapi, 4′,6-diamidino-2-phenylindole; MHC, myosin heavy chain; WT, wild type.

these data indicate that cyclin D3$^{-/-}$ satellite cells have a reduced proliferative potential in culture that reflects an impairment of cell cycle progression both at G1/S and G2/M phase transitions.

Finally, we assessed the differentiation capacity of cyclin D3-null primary myoblast by analyzing the expression of a number of muscle differentiation markers (Supporting Information Fig. S4A--S4C). No significant difference was detected

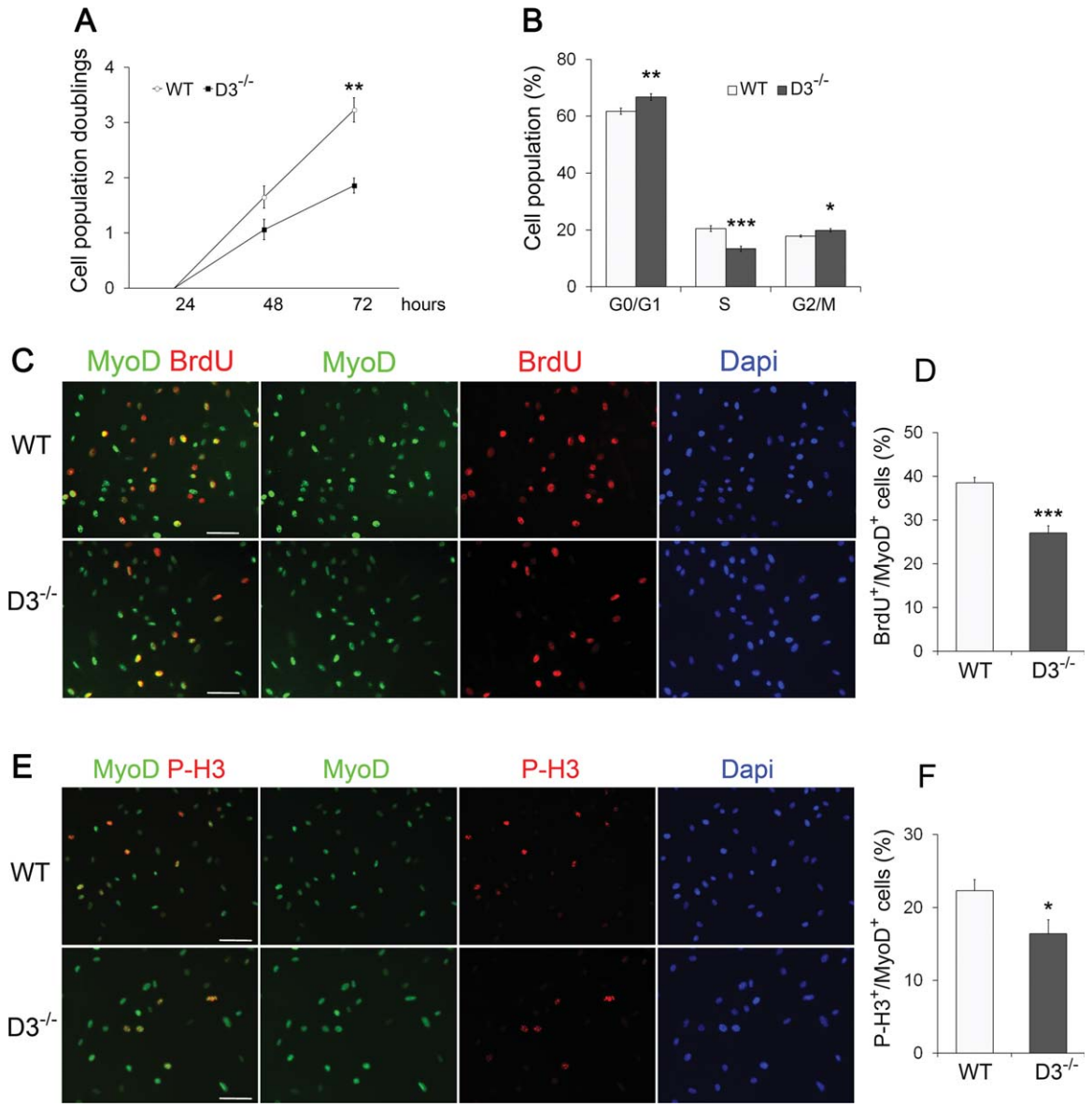

Figure 6. Cyclin D3 null satellite cells show proliferative deficits in vitro. **(A):** Primary myoblasts from dissociated limb muscles of WT and D3$^{-/-}$ mice were seeded in eight-well permanox chamber slides (10^4/well) and counted in 10 independent microscopic fields after 24, 48, and 72 hours in culture (>95% myogenic cells, as assessed by MyoD staining). The graph represents the mean number ± SEM ($n = 4$) of cell population doublings at 48 and 72 hours, relative to 24 hours (log 2 [number of cells at 48 or 72 hours]/number of cells at 24 hours). **(B):** WT and D3$^{-/-}$ primary myoblasts cultured for 48 hours were detached and stained with propidium iodide. Flow cytometry analysis of the cell cycle reveals a lower percentage of D3$^{-/-}$ cells in S-phase and a higher percentage in G0/G1 and G2/M compared with WT cells (means ± SEM, $n = 6$). **(C, E):** WT and D3$^{-/-}$ primary myoblasts cultured for 48 hours were labeled with 10 μM BrdU for 4 hours before fixation and immunostaining to detect BrdU (red), MyoD (green), and PH3 (red) as a marker of mitotic cells. Nuclei were counterstained with Dapi (blue). **(D, F):** The percentages of BrdU or P-H3 positive cells/total MyoD-positive cells are shown. Error bars represent ±SEM ($n = 4$). Asterisks denote significance (*, $p < .05$; **, $p < .01$; ***, $p < .001$). Scale bar = 50 μm. Abbreviations: Dapi, 4′,6-diamidino-2-phenylindole; P-H3, Phospho-Histone H3; WT, wild type.

between cyclin D3-null and WT differentiating myoblasts. Remarkably, however, cyclin D3-null myoblasts displayed decreased p21 protein expression, without a significant change of p21 mRNA levels, thus confirming the observation in C2.7 myoblasts depleted of cyclin D3 by RNA interference (Fig. 1).

Cyclin D3 Deficiency Affects Muscle Regenerative Capacity

In order to confirm that the above studies in vitro reflected the behavior of myogenic progenitor cells in vivo, acute injury was induced by injection of cardiotoxin into the TA muscle of age-matched cyclin D3$^{-/-}$ and WT mice. On day 3 after injury, mice were injected with BrdU intraperitoneally 6 hours before sacrifice and muscles were analyzed to determine the effects of cyclin D3 deficiency on proliferation and early differentiation of the satellite cell progeny. By costaining for the myogenic lineage marker MyoD and for BrdU, we were able to confirm in vivo that cyclin D3-null myogenic progenitors in the regenerating muscle displayed a significantly decreased proliferation rate compared to WT (Fig. 7A). Also, at this time point, there was a greater number of nascent

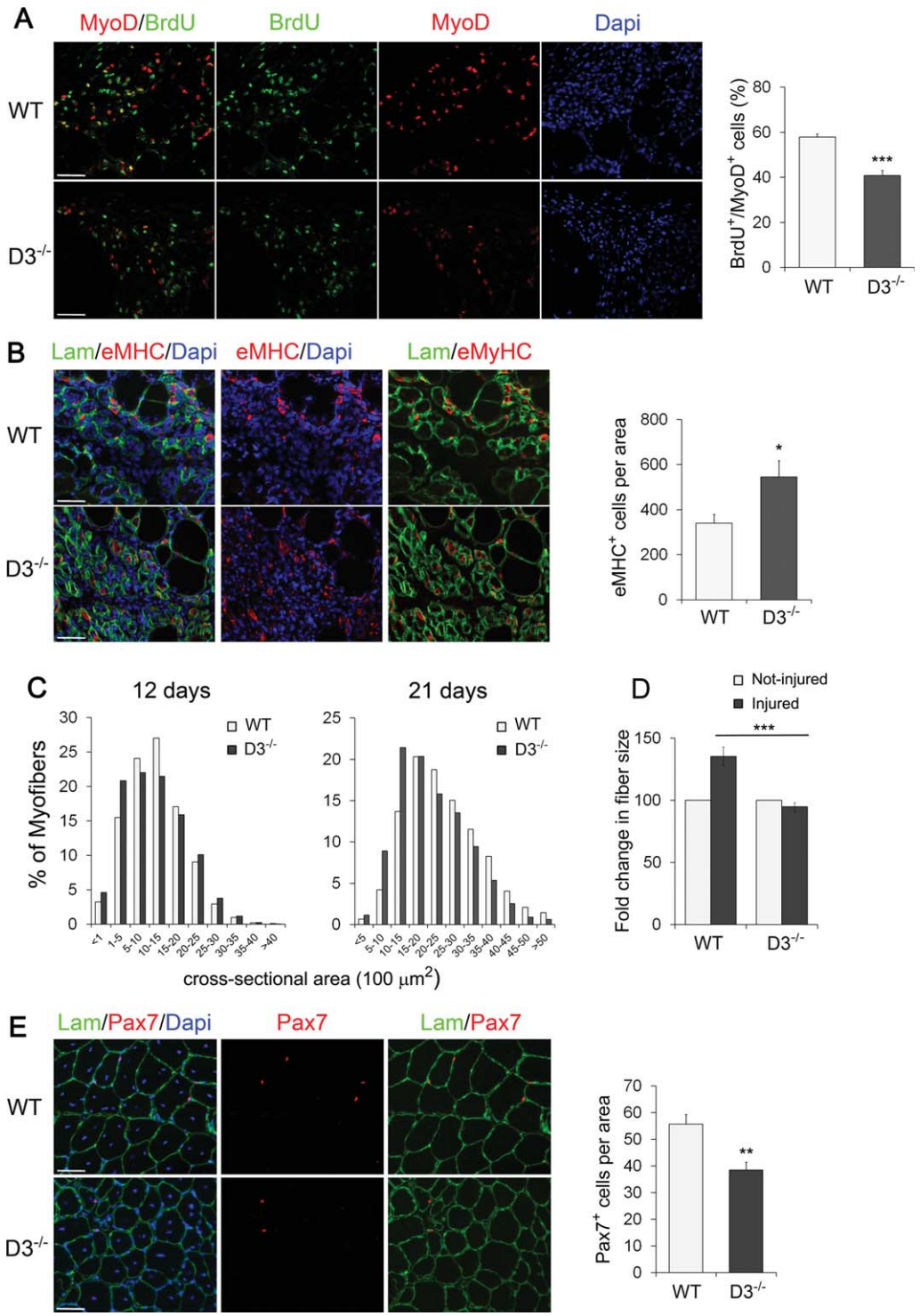

Figure 7. Loss of cyclin D3 affects muscle regeneration. **(A):** Acute muscle injury was induced in WT and D3$^{-/-}$ male mice at P60 by intramuscular injection of cardiotoxin. Mice were injected BrdU intraperitoneally 6 hours before sacrifice. Left, cross-sections of tibialis anterior (TA) muscles after 3 days of regeneration stained for MyoD (red) and BrdU (green) to label proliferating myogenic progenitors. Nuclei were counterstained with Dapi (blue). The graph on the right represents the mean percentage ± SEM of MyoD-positive cells that were BrdU^{+} (WT: $n = 5$; D3$^{-/-}$: $n = 4$). **(B)** Left, muscle cross-sections as in (A) were stained for eMHC (red) to identify newly generated myofibers and Laminin (green) to identify damaged fibers. Nuclei were counterstained with Dapi (blue). Right, quantitative analyses of nascent fiber number normalized to cross-sectional area of regenerating tissue (mean ± SEM for $n = 4$). **(C)** Frequency histograms showing the cross-sectional area of WT and cyclin D3-null myofibers 12 days and 21 days after cardiotoxin injection (12 days: $n = 3$; WT: 7,866 myofibers; D3$^{-/-}$: 7,633 myofibers—21 days: $n = 4$; WT: 4,826 myofibers; D3$^{-/-}$: 5,006 myofibers). **(D):** Fold change in regenerated fiber size from WT and D3$^{-/-}$ TA muscles 21 days after injury relative to uninjured fibers in adjacent areas of the tissue (means ± SEM, $n = 4$). **(E):** Left, cross-sections from regenerating TA muscles 21 days after injury stained for Pax7 (red) and Laminin (green). Nuclei were counterstained with Dapi (blue). Right, quantification of Pax7-positive cells associated with regenerated myofibers, normalized to 1 mm^2 of tissue cross-sectional area (means ± SEM; WT, $n = 5$; D3$^{-/-}$, $n = 3$). Asterisks denote significance (*, $p < .05$; **, $p < .01$; ***, $p < .001$). Scale bar = 50 μm. Abbreviations: Dapi, 4′,6-diamidino-2-phenylindole; eMHC, embryonic myosin heavy chain; Lam, Laminin; WT, wild type.

myotubes in cyclin D3-null muscles compared to control muscles, as determined by staining for embryonic myosin heavy-chain (eMHC) (Fig. 7B).

After 12 days from injury, cross-sectional area measurement indicated an increased number of smaller centrally nucleated myofibers in cyclin D3-null muscles compared to controls, presumably an effect of the reduced expansion and premature differentiation of myogenic precursors (Fig. 7C). Similarly, $D3^{-/-}$ muscles showed a decrease in myofiber size at 21 days of regeneration (Fig. 7C). Furthermore, assessment of the fiber cross-sectional area in both injured and uninjured areas of the muscle revealed that WT regenerated fibers displayed a 35% increase in fiber size relative to uninjured fibers, whereas cyclin $D3^{-/-}$ regenerated fibers were slightly smaller than uninjured fibers (Fig. 7D). At this time point, corresponding to the time by which self-renewal and homeostasis are being re-established, we also observed a reduced number of Pax7-positive cells associated with the regenerated myofibers (Fig. 7E). Collectively, these findings reveal that the absence of cyclin D3 in vivo results in reduced myogenic progenitor proliferation, precocious ability to differentiate into myofibers and depletion of self renewing cells, and are consistent with the effects observed in vitro.

Discussion

The mitogen-induced expression of D-type cyclins and assembly with their kinase partners are essential for adult stem cells to traverse the early G1 phase of the cell cycle, a sensitive period during which cells make the decision to enter S-phase or commit to differentiation [49]. Our study uncovers a nonredundant function played by cyclin D3 in controlling the proper developmental progression of adult myogenic precursors.

When compared with WT, adult cyclin D3-null muscles displayed a reduction in myofiber size, in the number of myofibers and in the number of satellite cells, suggesting that cyclin D3 deficiency affects postnatal muscle growth and impairs the establishment of the satellite cell population within adult muscle. The analysis of satellite cell behavior in vitro and their response to muscle injury in vivo provide direct evidence for a satellite cell defect in mice without cyclin D3.

Cyclin $D3^{-/-}$ myogenic progenitors in culture displayed reduced proliferative capacity and impaired G1/S progression indicating that cyclin D3 acts as a rate-limiting factor for transition through the G1 phase of the cell cycle. Myoblasts synthesize the three D-type cyclins whose common and major function is to phosphorylate and inactivate pRb in association with CDK4/6. The requirement for cyclin D3 could be a result of heterogeneity of myogenic precursors with respect to the expression of a specific cyclin D. Alternatively, cyclin D3 might possess additional nonredundant functions that contribute to promote G1/S progression and/or restrain the onset of differentiation. In this regard, a recent unbiased systematic substrate screen not only identified phosphorylation targets of CDK4/6 complexes additional to pRb but also revealed considerable difference between the cyclin D1-CDK4 and cyclin D3-CDK6 complex, with the latter phosphorylating a much broader spectrum of substrates [50]. Among the substrates that are preferentially phosphorylated by cyclin D3-based CDK complexes, we noticed a number of factors that are known to play critical functions in the control of myoblast proliferation and differentiation, including the DNA replication licensing factor CDC6 [19], the Polycomb methyltransferase Ezh2 [51], the transcriptional regulator MEF2D [52,53], and the inhibitor of differentiation ZEB1 [54].

In addition to G1/S progression, we found that cyclin D3 is also critical for G2/M phase transition. Previous work provided evidence that cyclin D3-CDK4 is active in S and G2 phases and that inhibiting this activity delays progression through the G2 phase and mitosis [55,56]. Furthermore, in the G2/M phase, cyclin D3 has been reported to interact with and act as a regulatory subunit of CDK-11^{p58}/ $p58^{PITSLRE}$, a G2/M CDK [57].

Similarly to that observed in cyclin D3-null primary myoblasts, asynchronously proliferating C2 myoblasts depleted of cyclin D3 by RNA-interference exhibited impaired G1/S progression, whereas the residual expression of cyclin D3 was sufficient to efficiently drive these cells through the G2/M transition. Furthermore, compared with controls, cyclin D3-depleted myoblasts displayed enhanced expression of MyoD, anticipated exit from the cell cycle in low-mitogen medium, and earlier differentiation. The higher levels of MyoD probably reflect the increased fraction of cells in G1; in fact, MyoD expression is known to be regulated in a cell cycle-dependent manner reaching its highest level in G1 phase, the time-window during which myoblasts can exit the cell cycle to enter differentiation [58]. An anticipated timing of differentiation was not appreciable in cyclin D3-null primary myoblasts compared with WT controls, probably due to the high propensity of primary myoblasts to undergo spontaneous differentiation even if cultured in high-mitogen medium.

However, the analysis of myofiber-associated satellite cells in culture revealed that the clusters of satellite cell progeny resident on cycD3-null myofibers were smaller in size and contained an increased number of differentiating cells, with a reciprocal decrease in self-renewing cells. Furthermore, cyclin D3 deficiency impaired the generation of undifferentiated $Pax7^{+}$ "reserve cells" following terminal differentiation of myofiber-derived plated satellite cells.

A similar behavior was exhibited by cyclin D3-null satellite cells activated in vivo following injury-induced muscle regeneration. In fact, during the early phase of regeneration, cyclin D3-null myogenic progenitors displayed a reduced proliferative capacity and a concomitantly increased propensity for differentiation, whereas at the end of the regeneration process, the size of regenerated fibers was smaller in cyclin D3-null muscle than in WT, and the number of $Pax7^{+}$ cells repopulating the satellite cell niche was reduced.

Therefore, cyclin D3 appears to function by stimulating proliferation and preventing precocious differentiation of satellite cells, thus allowing full expansion of transit-amplifying myogenic progenitors and preserving the self-renewing population. This may rely on its known ability to facilitate a rapid transition through the G1 phase, a crucial period during which the cells are susceptible to cell-cycle exit and commitment to differentiation. An additional possibility, that needs to be investigated, is that cyclin D3 may play a cell cycle-independent function in transcriptional regulation of myogenic differentiation genes.

Notably, the defects of cyclin D3-null satellite cells are similar to those displayed by satellite cells with disrupted function of the Polycomb proteins Ezh2 or Bmi1 [51,59]. Indeed, Polycomb complexes are known to play a pivotal role in maintaining the self-renewal capability of various adult stem cells by binding directly and repressing the promoter of p16, a specific inhibitor of the activity of cyclin D-dependent kinases [60–64].

Our results highlight a critical requirement of cyclin D3 in maintaining the proliferative potential of myogenic progenitors; this extends the reported crucial role of cyclin D3 for

the proliferative expansion of specific progenitor populations within several hematopoietic lineages, including immature T lymphocytes, early B cells, germinal center B cells, granulocytes, and terminally differentiating erythroid precursors [26,65–69]. In these cell types, specific extrinsic and intrinsic signals dictate the expression of cyclin D3, whereas the other D cyclins are not expressed or nonfunctional. Importantly, in pro-B cells and in myeloid progenitor cells, in addition to promoting cell cycle progression, cyclin D3 has been recognized to play a function in transcriptional regulation of differentiation-specific programs [70–72].

In contrast to cyclin D1 and D2, cyclin D3 mRNA expression is induced in C2 myoblasts transitioning from proliferation to differentiation. A recent analysis of differentiating MyoD-null primary myoblasts confirmed that cyclin D3 mRNA levels are sustained by MyoD, whereas at the same time MyoD mediates downregulation of cyclin D1 and D2 transcripts [15]. The regulation of cyclin D3 expression during myogenic progression in vitro, combined with the results presented here, suggests that cyclin D3 may function to integrate environmental cues with intrinsic signals to selectively expand myogenic precursors at a specific transitional stage, or a distinctly specified subset of progenitors, where the other D-type cyclins are repressed.

Myoblasts must irreversibly exit the cell cycle to initiate differentiation and this is achieved through induction of the p21 and p57 cyclin-dependent kinase inhibitors [73]. Previously, we have shown that cyclin D3 protein accumulates in differentiated myotubes by forming kinase-inactive complexes with CDK4 and p21 and mediating their interaction with unphosphorylated pRb [18,39].

Here, we found that differentiating myocytes lacking cyclin D3 express substantially reduced levels of p21 protein, but not p21 mRNA, revealing that cyclin D3 promotes p21 protein synthesis or stabilization. Thus, in addition to stimulating proliferation, cyclin D3 appears to participate in the process arresting the cell cycle and favoring differentiation.

It has been recently reported that an adenovirus-mediated upregulation of cyclin D3 in C2C12 myoblasts results in premature entrance in the myogenic differentiation program, which appears to contrast with our results showing a similar phenotypic consequence of cyclin D3 ablation. However, in agreement with our results, cyclin D3-overexpressing myoblasts were also shown to exhibit an elevated expression of p21, at the protein but not at the mRNA level, and an enhanced cell cycle exit, which might explain their faster differentiation kinetics [74]. Further, ectopic expression of cyclin D3 was shown to correct early steps of differentiation in primary myoblasts from myotonic dystrophy type 1 patients and this was ascribed to cyclin D3/CDK4/6-mediated phosphorylation and activation of CUGBP1, a key regulator of translation of proteins involved in muscle differentiation, including p21 and MEF2A [75–77].

Conclusion

This study establishes cyclin D3 as a critical regulator of proliferation and self-renewal of myogenic progenitors. Cyclin D3 also appears to promote the accumulation of p21 in differentiating myocytes thus providing a negative autoregulatory loop that contributes to switch myogenic cells to terminal differentiation.

Acknowledgments

We thank Piotr Sicinski (Dana Farber Cancer Institute, Boston, MA) for kindly providing cyclin D3 knockout mice and Livio Baron for excellent technical assistance. This work was supported by funding to M.C. from the Telethon Foundation (Grant GGP08126). G.D.L. was partially supported by Filas-Regione Lazio. M.B. is currently affiliated with the Institute of Functional Genomics, CNRS-Inserm, Montpellier, France. E.M. is currently affiliated with the Virginia Commonwealth University, School of Pharmacy, Richmond, VA.

Disclosure of Potential Conflicts of Interest

The authors indicate no potential conflicts of interest.

References

1 Collins CA, Olsen I, Zammit PS et al. Stem cell function, self-renewal, and behavioral heterogeneity of cells from the adult muscle satellite cell niche. Cell 2005;122:289–301.
2 Zammit PS. All muscle satellite cells are equal, but are some more equal than others? J Cell Sci 2008;121(Pt 18):2975–2982.
3 Kuang S, Gillespie MA, Rudnicki MA. Niche regulation of muscle satellite cell self-renewal and differentiation. Cell Stem Cell 2008;2:22–31.
4 Brack AS, Rando TA. Tissue-specific stem cells: Lessons from the skeletal muscle satellite cell. Cell Stem Cell 2012;10:504–514.
5 Wang YX, Rudnicki MA. Satellite cells, the engines of muscle repair. Nat Rev Mol Cell Biol 2012;13:127–133.
6 Megeney LA, Kablar B, Garrett K et al. MyoD is required for myogenic stem cell function in adult skeletal muscle. Genes Dev 1996;10:1173–1183.
7 Montarras D, Lindon C, Pinset C et al. Cultured myf5 null and myoD null muscle precursor cells display distinct growth defects. Biol Cell 2000;92:565–572.
8 Macharia R, Otto A, Valasek P et al. Neuromuscular junction morphology, fiber-type proportions, and satellite-cell proliferation rates are altered in MyoD(-/-) mice. Muscle Nerve 2010;42:38–52.
9 Sabourin LA, Girgis-Gabardo A, Seale P et al. Reduced differentiation potential of primary MyoD-/- myogenic cells derived from adult skeletal muscle. J Cell Biol 1999;144:631–643.
10 Yablonka-Reuveni Z, Rudnicki MA, Rivera AJ et al. The transition from proliferation to differentiation is delayed in satellite cells from mice lacking MyoD. Dev Biol 1999;210:440–455.
11 Kitzmann M, Fernandez A. Crosstalk between cell cycle regulators and the myogenic factor MyoD in skeletal myoblasts. Cell Mol Life Sci 2001;58:571–579.
12 Halevy O, Novitch BG, Spicer DB et al. Correlation of terminal cell cycle arrest of skeletal muscle with induction of p21 by MyoD. Science 1995;267:1018–1021.
13 Magenta A, Cenciarelli C, De Santa F et al. MyoD stimulates RB promoter activity via the CREB/p300 nuclear transduction pathway. Mol Cell Biol 2003;23:2893–2906.
14 Busanello A, Battistelli C, Carbone M et al. MyoD regulates p57kip2 expression by interacting with a distant cis-element and modifying a higher order chromatin structure. Nucleic Acids Res 2012;40:8266–8275.
15 Parker MH, von Maltzahn J, Bakkar N et al. MyoD-dependent regulation of NF-kappaB activity couples cell-cycle withdrawal to myogenic differentiation. Skelet Muscle 2012;2:6.
16 Micheli L, Leonardi L, Conti F et al. PC4/Tis7/IFRD1 stimulates skeletal muscle regeneration and is involved in myoblast differentiation as a regulator of MyoD and NF-kappaB. J Biol Chem 2011;286:5691–5707.
17 Kiess M, Montgomery Gill R, Hamel PA. Expression of the positive regulator of cell cycle progression, cyclin D3, is induced during differentiation of myoblasts into quiescent myotubes. Oncogene 1995;10:159–166.

18 Cenciarelli C, De Santa F, Puri PL et al. Critical role played by cyclin D3 in the MyoD-mediated arrest of cell cycle during myoblast differentiation. Mol Cell Biol 1999;19:5203–5217.
19 Zhang K, Sha J, Harter ML. Activation of Cdc6 by MyoD is associated with the expansion of quiescent myogenic satellite cells. J Cell Biol 2010;188:39–48.
20 Sherr CJ. D-type cyclins. Trends Biochem Sci 1995;20:187–190.
21 Dyson N. The regulation of E2F by pRB-family proteins. Genes Dev 1998;12:2245–2262.
22 Sherr CJ, Roberts JM. CDK inhibitors: Positive and negative regulators of G1-phase progression. Genes Dev 1999;13:1501–1512.
23 Fantl V, Stamp G, Andrews A et al. Mice lacking cyclin D1 are small and show defects in eye and mammary gland development. Genes Dev 1995;9:2364–2372.
24 Sicinski P, Donaher JL, Parker SB et al. Cyclin D1 provides a link between development and oncogenesis in the retina and breast. Cell 1995;82:621–630.
25 Sicinski P, Donaher JL, Geng Y et al. Cyclin D2 is an FSH-responsive gene involved in gonadal cell proliferation and oncogenesis. Nature 1996;384:470–474.
26 Sicinska E, Aifantis I, Le Cam L et al. Requirement for cyclin D3 in lymphocyte development and T cell leukemias. Cancer Cell 2003;4:451–461.
27 Ciemerych MA, Kenney AM, Sicinska E et al. Development of mice expressing a single D-type cyclin. Genes Dev 2002;16:3277–3289.
28 Kozar K, Ciemerych MA, Rebel VI et al. Mouse development and cell proliferation in the absence of D-cyclins. Cell 2004;118:477–491.
29 Paternot S, Arsenijevic T, Coulonval K et al. Distinct specificities of pRb phosphorylation by CDK4 activated by cyclin D1 or cyclin D3: Differential involvement in the distinct mitogenic modes of thyroid epithelial cells. Cell Cycle 2006;5:61–70.
30 Coqueret O. Linking cyclins to transcriptional control. Gene 2002;299:35–55.
31 Lazaro JB, Bailey PJ, Lassar AB. Cyclin D-cdk4 activity modulates the subnuclear localization and interaction of MEF2 with SRC-family coactivators during skeletal muscle differentiation. Genes Dev 2002;16:1792–1805.
32 Despouy G, Bastie JN, Deshaies S et al. Cyclin D3 is a cofactor of retinoic acid receptors, modulating their activity in the presence of cellular retinoic acid-binding protein II. J Biol Chem 2003;278:6355–6362.
33 Liu W, Sun M, Jiang J et al. Cyclin D3 interacts with human activating transcription factor 5 and potentiates its transcription activity. Biochem Biophys Res Commun 2004;321:954–960.
34 Sarruf DA, Iankova I, Abella A et al. Cyclin D3 promotes adipogenesis through activation of peroxisome proliferator-activated receptor gamma. Mol Cell Biol 2005;25:9985–9995.
35 Bienvenu F, Jirawatnotai S, Elias JE et al. Transcriptional role of cyclin D1 in development revealed by a genetic-proteomic screen. Nature 2010;463:374–378.
36 Jahn L, Sadoshima J, Izumo S. Cyclins and cyclin-dependent kinases are differentially regulated during terminal differentiation of C2C12 muscle cells. Exp Cell Res 1994;212:297–307.
37 Rao SS, Chu C, Kohtz DS. Ectopic expression of cyclin D1 prevents activation of gene transcription by myogenic basic helix-loop-helix regulators. Mol Cell Biol 1994;14:5259–5267.
38 Rao SS, Kohtz DS. Positive and negative regulation of D-type cyclin expression in skeletal myoblasts by basic fibroblast growth factor and transforming growth factor beta. A role for cyclin D1 in control of myoblast differentiation. J Biol Chem 1995;270:4093–4100.
39 De Santa F, Albini S, Mezzaroma E et al. pRb-dependent cyclin D3 protein stabilization is required for myogenic differentiation. Mol Cell Biol 2007;27:7248–7265.
40 Skapek SX, Rhee J, Spicer DB et al. Inhibition of myogenic differentiation in proliferating myoblasts by cyclin D1-dependent kinase. Science 1995;267:1022–1024.
41 Skapek SX, Rhee J, Kim PS et al. Cyclin-mediated inhibition of muscle gene expression via a mechanism that is independent of pRB hyperphosphorylation. Mol Cell Biol 1996;16:7043–7053.
42 Bartkova J, Lukas J, Strauss M et al. Cyclin D3: Requirement for G1/S transition and high abundance in quiescent tissues suggest a dual role in proliferation and differentiation. Oncogene 1998;17:1027–1037.
43 Tseng BS, Zhao P, Pattison JS et al. Regenerated mdx mouse skeletal muscle shows differential mRNA expression. J Appl Physiol 2002;93:537–545.
44 Pinset C, Montarras D, Chenevert J et al. Control of myogenesis in the mouse myogenic C2 cell line by medium composition and by insulin: Characterization of permissive and inducible C2 myoblasts. Differentiation 1988;38:28–34.
45 Paddison PJ, Cleary M, Silva JM et al. Cloning of short hairpin RNAs for gene knockdown in mammalian cells. Nat Methods 2004;1:163–167.
46 Dickins RA, Hemann MT, Zilfou JT et al. Probing tumor phenotypes using stable and regulated synthetic microRNA precursors. Nat Genet 2005;37:1289–1295.
47 Chomczynski P, Sacchi N. Single-step method of RNA isolation by acid guanidinium thiocyanate-phenol-chloroform extraction. Anal Biochem 1987;162:156–159.
48 Zammit PS, Golding JP, Nagata Y et al. Muscle satellite cells adopt divergent fates: A mechanism for self-renewal? J Cell Biol 2004;166:347–357.
49 Orford KW, Scadden DT. Deconstructing stem cell self-renewal: Genetic insights into cell-cycle regulation. Nat Rev Genet 2008;9:115–128.
50 Anders L, Ke N, Hydbring P et al. A systematic screen for CDK4/6 substrates links FOXM1 phosphorylation to senescence suppression in cancer cells. Cancer Cell 2011;20:620–634.
51 Juan AH, Derfoul A, Feng X et al. Polycomb EZH2 controls self-renewal and safeguards the transcriptional identity of skeletal muscle stem cells. Genes Dev 2011;25:789–794.
52 Penn BH, Bergstrom DA, Dilworth FJ et al. A MyoD-generated feed-forward circuit temporally patterns gene expression during skeletal muscle differentiation. Genes Dev 2004;18:2348–2353.
53 Rampalli S, Li L, Mak E et al. p38 MAPK signaling regulates recruitment of Ash2L-containing methyltransferase complexes to specific genes during differentiation. Nat Struct Mol Biol 2007;14:1150–1156.
54 Postigo AA, Dean DC. ZEB, a vertebrate homolog of Drosophila Zfh-1, is a negative regulator of muscle differentiation. EMBO J 1997;16:3935–3943.
55 Gabrielli BG, Sarcevic B, Sinnamon J et al. A cyclin D-Cdk4 activity required for G2 phase cell cycle progression is inhibited in ultraviolet radiation-induced G2 phase delay. J Biol Chem 1999;274:13961–13969.
56 Burgess A, Wigan M, Giles N et al. Inhibition of S/G2 phase CDK4 reduces mitotic fidelity. J Biol Chem 2006;281:9987–9995.
57 Zhang S, Cai M, Zhang S et al. Interaction of p58(PITSLRE), a G2/M-specific protein kinase, with cyclin D3. J Biol Chem 2002;277:35314–35322.
58 Kitzmann M, Carnac G, Vandromme M et al. The muscle regulatory factors MyoD and myf-5 undergo distinct cell cycle-specific expression in muscle cells. J Cell Biol 1998;142:1447–1459.
59 Robson LG, Di Foggia V, Radunovic A et al. Bmi1 is expressed in postnatal myogenic satellite cells, controls their maintenance and plays an essential role in repeated muscle regeneration. PLoS One 2011;6:e27116.
60 Chen H, Gu X, Su IH et al. Polycomb protein Ezh2 regulates pancreatic beta-cell Ink4a/Arf expression and regeneration in diabetes mellitus. Genes Dev 2009;23:975–985.
61 Ezhkova E, Pasolli HA, Parker JS et al. Ezh2 orchestrates gene expression for the stepwise differentiation of tissue-specific stem cells. Cell 2009;136:1122–1135.
62 Pereira JD, Sansom SN, Smith J et al. Ezh2, the histone methyltransferase of PRC2, regulates the balance between self-renewal and differentiation in the cerebral cortex. Proc Natl Acad Sci USA 2010;107:15957–15962.
63 Bruggeman SW, van Lohuizen M. Controlling stem cell proliferation: CKIs at work. Cell Cycle 2006;5:1281–1285.
64 Molofsky AV, He S, Bydon M et al. Bmi-1 promotes neural stem cell self-renewal and neural development but not mouse growth and survival by repressing the p16Ink4a and p19Arf senescence pathways. Genes Dev 2005;19:1432–1437.
65 Cooper AB, Sawai CM, Sicinska E et al. A unique function for cyclin D3 in early B cell development. Nat Immunol 2006;7:489–497.
66 Peled JU, Yu JJ, Venkatesh J et al. Requirement for cyclin D3 in germinal center formation and function. Cell Res 2010;20:631–646.
67 Cato MH, Chintalapati SK, Yau IW et al. Cyclin D3 is selectively required for proliferative expansion of germinal center B cells. Mol Cell Biol 2011;31:127–137.
68 Sicinska E, Lee YM, Gits J et al. Essential role for cyclin D3 in granulocyte colony-stimulating factor-driven expansion of neutrophil granulocytes. Mol Cell Biol 2006;26:8052–8060.
69 Sankaran VG, Ludwig LS, Sicinska E et al. Cyclin D3 coordinates the cell cycle during differentiation to regulate erythrocyte size and number. Genes Dev 2012;26:2075–2087.
70 Powers SE, Mandal M, Matsuda S et al. Subnuclear cyclin D3 compartments and the coordinated regulation of proliferation and immunoglobulin variable gene repression. J Exp Med 2012;209:2199–2213.
71 Peterson LF, Boyapati A, Ranganathan V et al. The hematopoietic transcription factor AML1 (RUNX1) is negatively regulated by the cell cycle protein cyclin D3. Mol Cell Biol 2005;25:10205–10219.
72 Kato JY, Sherr CJ. Inhibition of granulocyte differentiation by G1 cyclins D2 and D3 but not D1. Proc Natl Acad Sci USA 1993;90:11513–11517.
73 Zhang P, Wong C, Liu D et al. p21(CIP1) and p57(KIP2) control muscle differentiation at the myogenin step. Genes Dev 1999;13:213–224.

74 Gurung R, Parnaik VK. Cyclin D3 promotes myogenic differentiation and Pax7 transcription. J Cell Biochem 2012;113:209–219.
75 Salisbury E, Sakai K, Schoser B et al. Ectopic expression of cyclin D3 corrects differentiation of DM1 myoblasts through activation of RNA CUG-binding protein, CUGBP1. Exp Cell Res 2008;314:2266–2278.
76 Timchenko NA, Iakova P, Cai ZJ et al. Molecular basis for impaired muscle differentiation in myotonic dystrophy. Mol Cell Biol 2001;21:6927–6938.
77 Timchenko NA, Patel R, Iakova P et al. Overexpression of CUG triplet repeat-binding protein, CUGBP1, in mice inhibits myogenesis. J Biol Chem 2004;279:13129–13139.

See www.StemCells.com for supporting information available online.

Caruso Figure S1 “top”

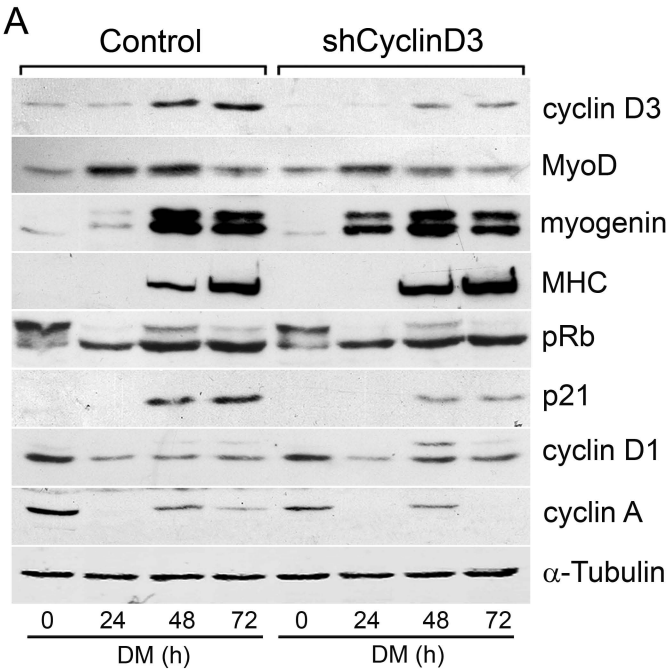

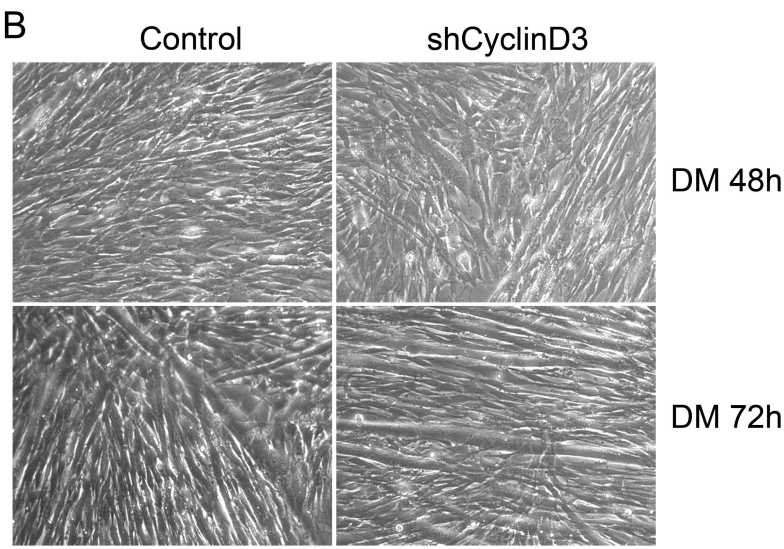

Caruso Figure S2 “top”

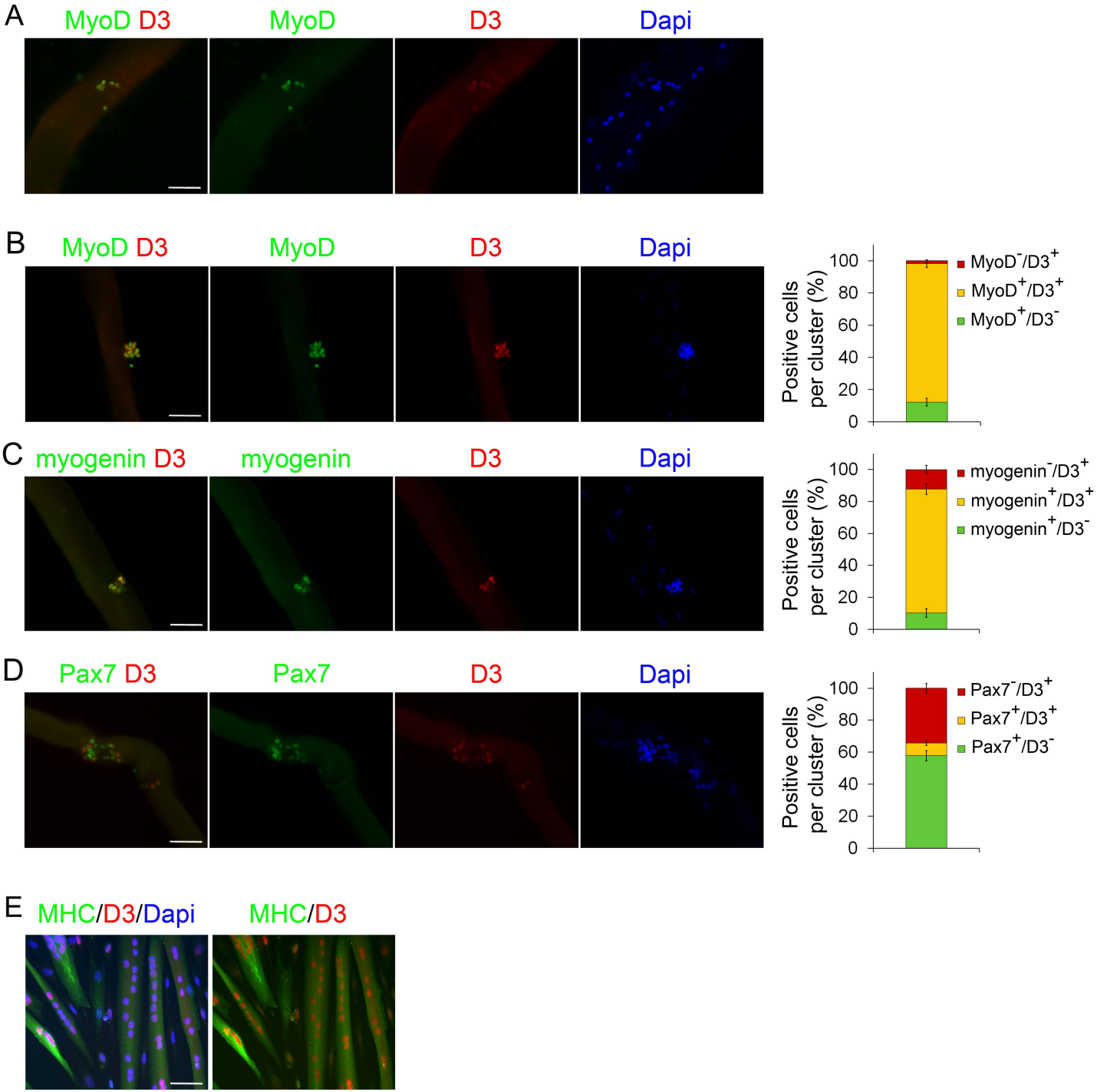

Caruso Figure S3 “top”

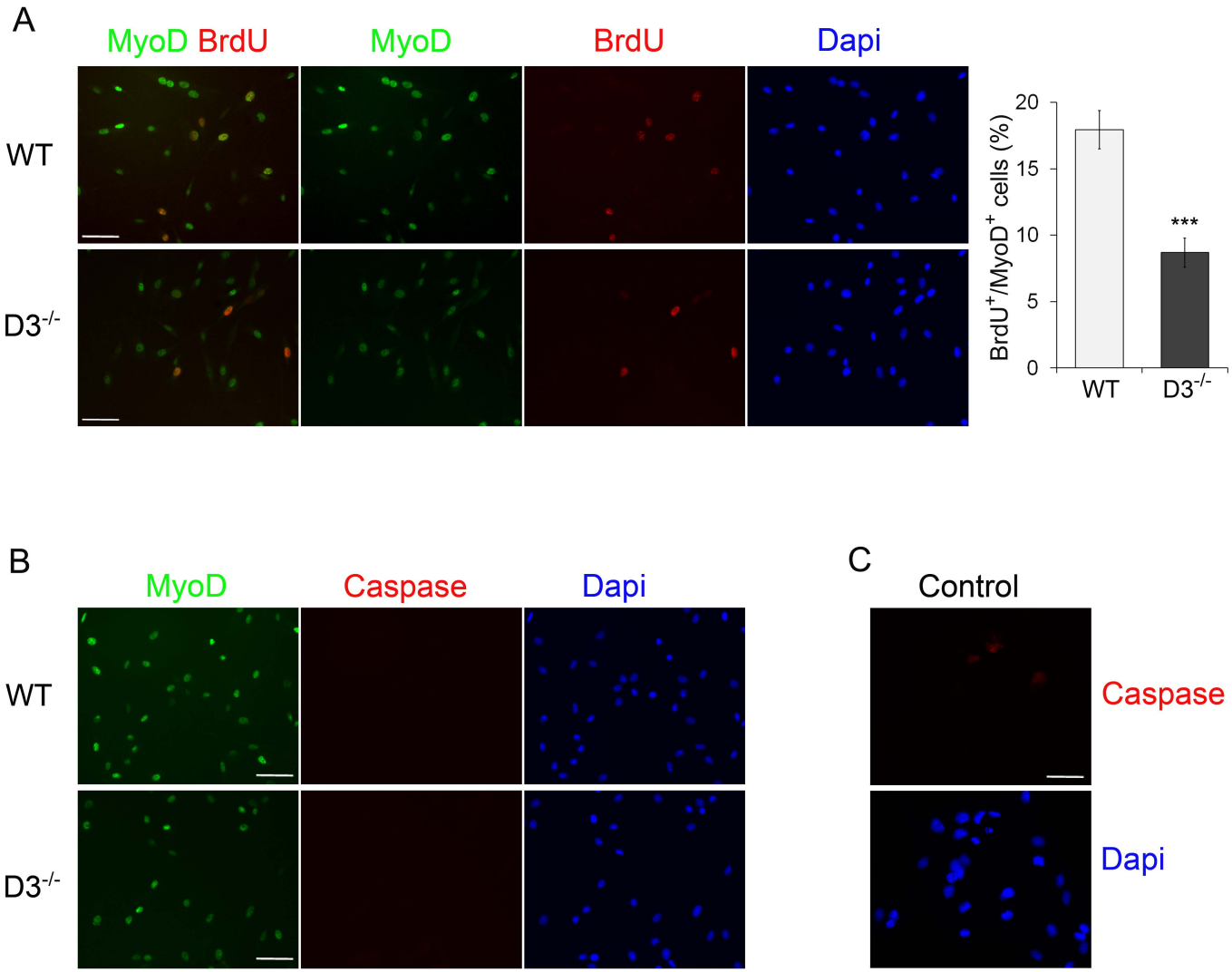

Caruso Figure S4 “top”

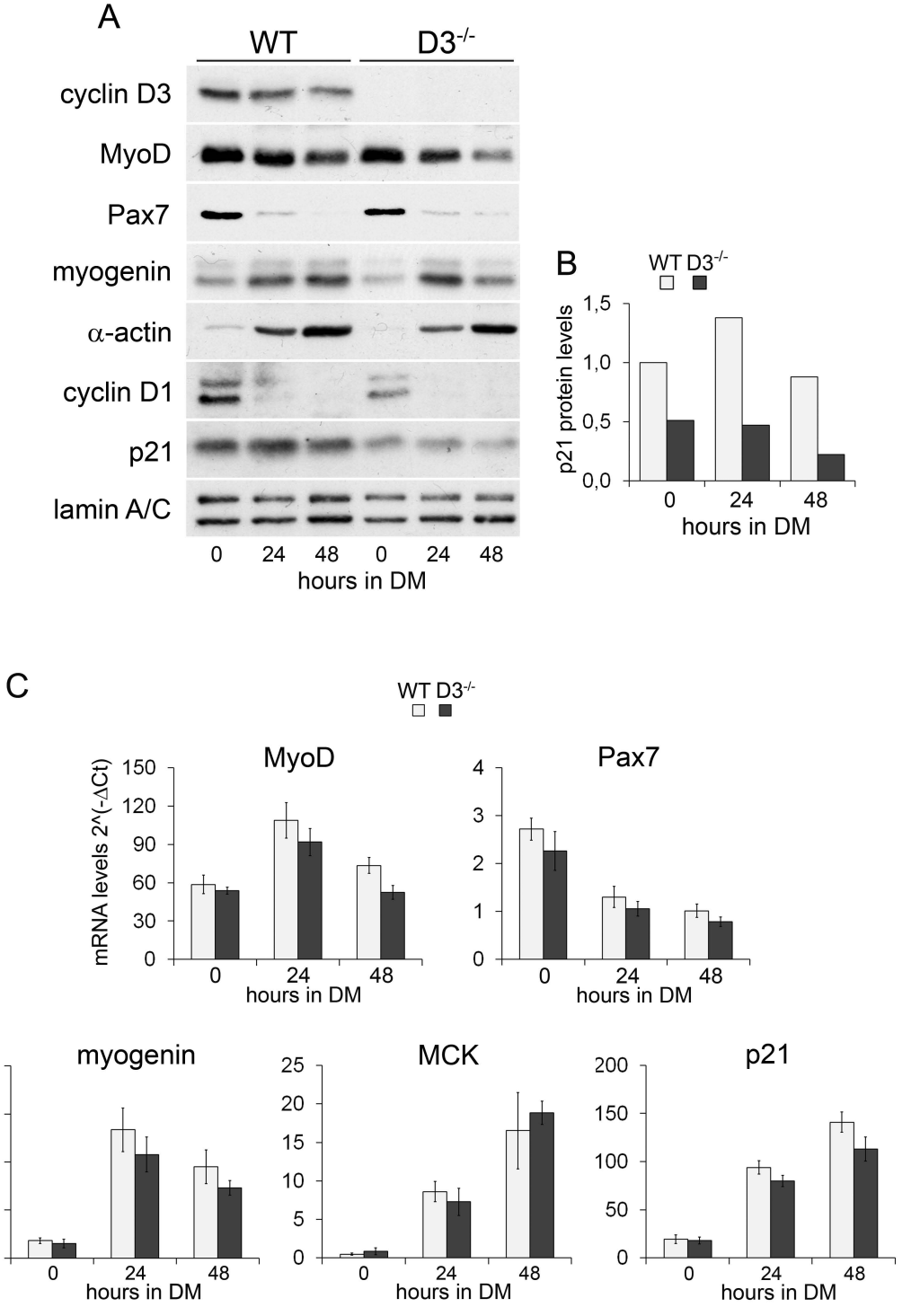

Figure S1. Cyclin D3 knockdown in myoblasts does not impair myotube formation in a context of high cell density

C2.7 myoblasts transduced either with the retrovirus expressing cyclin D3-specific shRNA (shCyclin D3) or with the empty retrovirus (control) were seeded at $3x10^6$ cells into 90-mm dishes, and transferred to differentiation medium (DM) after 5 hours. Whole cell extracts were prepared from cells collected at indicated times after exposure to DM. **A)** Western blot analysis was performed using antibodies specific for the indicated proteins. **B)** Phase-contrast microphotographs (whole 20x field) showing cells induced to differentiate for 2-3 days

Figure S2. Analysis of cyclin D3 expression in myofiber-associated or plated satellite cells

A) EDL myofibers were cultured in suspension for 48 hours and then coimmunostained for cyclin D3 (red) and MyoD (green) and counterstained with DAPI (blue).

B, C, D) EDL myofibers cultured in suspension for 72 hours were coimmunostained for cyclin D3 (red) and MyoD (green), cyclin D3 (red) and myogenin (green), or cyclin D3 (red) Pax7 (green), as indicated. Counterstaining with DAPI was used to identify all nuclei present on the myofiber. The graphs on the right represent the quantification of cells contained in clusters of 4 or more cells that stained positive for the indicated proteins. Data era expressed as the percentage in each category of the total positive cells per cluster (means ± SEM). Results are from three independent myofiber preparations; at least 20 clusters were analyzed for each coimmunofluorescence (D3-MyoD, D3-myogenin or D3-Pax7) and for each experiment. **E)** Satellite cells derived from EDL myofibers plated on matrigel coated chamber slides were cultured for 3 days in growth medium and then induced to differentiate in low-mitogen medium for 72 hours before fixing and immunostaining for cyclin D3 (red) and myosin heavy chain (MCH, green). Counterstaining with DAPI was used to visualize all nuclei. Scale bar= 50 μm.

Figure S3. Loss of cyclin D3 does not lead to apoptosis

A) Equal numbers of satellite cells derived from WT and $D3^{-/-}$ EDL myofibers were plated in 8-well permanox chamber slides ($8x10^3$/well), cultured for 48 hours, and then labeled with BrdU for 2 hours before fixation and immunostaining for BrdU (red) and MyoD (green). Nuclei were counterstained with DAPI (blue). The graph on the left represents the average percentage of BrdU-positive cells of the total MyoD-positive cells. Error bars represent ±SEM (WT: n=6; $D3^{-/-}$: n=7). Asterisks denote significance (***p>0.001). **B**) The same cells as in **A**) were examined for apoptosis by coimmunostaining for activated Caspase-3 (red) and MyoD (green). **C**) C2.7 myoblasts treated with cisplatinum for 24 hours prior to fixation served as positive control for Caspase staining (red). Nuclei were counterstained with DAPI (blue). Scale bar= 50 μm.

Figure S4. Gene expression analysis of WT and cyclin D3-null primary myoblasts

A) WT and $D3^{-/-}$ primary myoblasts from dissociated limb muscles were seeded at $5x10^5$ cells into 60-mm dishes and shifted to DM after 24 hours. Cells were collected 24 hours after seeding (DM 0 hours) or at the indicated times after exposure to DM. Whole cell extracts were subjected to western blot analysis using the indicated antibodies. **B**) Quantification of p21 protein levels by densitometry analysis of the western blot shown in A); values are presented as fold change relative to control myoblasts at the DM 0 time point (set to 1), after normalization to the corresponding values of lamin A/C levels. **C)** RT- qPCR analysis was performed on genes indicated. Data are expressed as mRNA levels relative to TBP. Graphs represent average 2^-ΔCT values ± SEM (n=4).

Table S1

Antibody	Clone	Ig type	Conjugate	Supplier	Application and dilution
Primary antibodies					
Cyclin D3	C-16 polyclonal	Rabbit IgG	-	Santa Cruz	WB, 1:400
MyoD	5.8A	Mouse IgG1	-	Dako	WB, 1:500 IF, 1:100-1:200
myogenin	F5D	Mouse IgG1	-	DHSB	WB, 1:18
MHC	MF20	Mouse IgG2b	-	DHSB	WB, 1:25 IF, 1:10
Sarcomeric α-actin	5C5	Mouse IgG	-	Sigma	WB, 1:5000
Rb	G3-245	Mouse IgG1	-	Pharmigen	WB, 1:1000
p21	C-19 polyclonal	Rabbit IgG	-	Santa Cruz	WB, 1:250
Cyclin D1	72-13G	Mouse IgG1	-	Santa Cruz	WB, 1:200
α-Tubulin	DM 1A	Mouse IgG1	-	Sigma	WB, 1:10000
Cyclin A	C-19 polyclonal	Rabbit IgG	-	Santa Cruz	WB, 1:400
Lamin A/C	N-18 polyclonal	Goat IgG	-	Santa Cruz	WB, 1:1000

BrdU	BU1/75 (ICR1)	Rat IgG2A	-	Serotec	IF, 1:300-1:1000
Phospho-Histone H3 (Ser10)	polyclonal	Rabbit IgG	-	Millipore	IF, 1:500
Pax7	Pax7	Mouse IgG1	-	DHSB	WB - IF, 1:3-1:10
myogenin	M-225 polyclonal	Rabbit IgG	-	Santa Cruz	IF, 1:200
MyoD	C-20 polyclonal	Rabbit IgG	-	Santa Cruz	IF, 1:300 WB, 1:800
Laminin	polyclonal	Rabbit IgG	-	Sigma	IF, 1:400
eMyHC	F1.652	Mouse IgG1	-	DSHB	IF, 1:25
Cyclin D3	18B6-10	Rat IgG2a	-	Santa Cruz	IF, 1:75
Cyclin D3	DCS-22	Mouse IgG1	-	Santa Cruz	IF,1:100
Cleaved Caspase-3 (Asp175)	polyclonal	Rabbit IgG	-	Cell signaling	IF, 1:1000
Secondary antibodies					
Rabbit IgG	-	Goat	Alexa Fluor 488	Molecular Probes	IF, 1:1000
Rabbit IgG	-	Donkey	Alexa Fluor 555	Molecular Probes	IF, 1:1000
Mouse IgG	-	Goat	Alexa Fluor 488	Molecular Probes	IF, 1:1000
Mouse IgG	-	Goat	Alexa Fluor 594	Molecular Probes	IF, 1:1000

Mouse IgG2b	-	Goat	Alexa Fluor 488	Molecular Probes	IF, 1:1000
Mouse IgG1	-	Goat	Biotin	Jackson	IF, 1:1000
Rat	-	Donkey	Cy2	Jackson	IF, 1:150
Rat IgG	-	Donkey	TRITC	Jackson	IF, 1:300
Rabbit IgG	-	Donkey	Peroxidase	Jackson	WB, 1:20000
Mouse IgG	-	Donkey	Peroxidase	Jackson	WB, 1:20000
Goat IgG	-	Donkey	Peroxidase	Jackson	WB, 1:20000
DHSB, Developmental Studies Hybridoma Bank; IF, immunofluorescence; WB, western blot					

Table S2

Target	Seq ID	Primers	UPL Roche #
MyoD	M18779.1	F- tcacagcgaaggccactt R- gccactcaaggatcagctct	#71
MCK	NM_007710.1	F- cagcacagacagacactcagg R- gaacttgttgtgggtgttgc	#20
Myogenin	NM_031189.1	F- ccttgctcagctccctca R- tgggagttgcattcactgg	#63
Pax7	NM_011039.1	F- ggcacagaggaccaagctc R- gcacgccggttactgaac	#85
MHC	XM_354614	F- ggatgggaaagtcactgtgg R- gtcctctggcttaaccacca	#18
p21	NM_007669.2	F- tccacagcgatatccagaca R- ggacatcaccaggattggac	#21
Rb	NM_009029.1	F- gagctcatgagagaccgaca R- caccttgcagatgccataca	#93
Cyclin D3	NM_007632.2	F- ggaagatgctggcatactgg R- ccaggtagttcatagccagagg	#101
Cyclin D1	NM_007631.2	F- gagattgtgccatccatgc R- ctcctcttcgcacttctgct	#67
Cyclin A	NM_009828.2	F- cttggctgcaccaacagtaa R- caaactcagttctcccaaaaaca	#4
TBP	NM_013684.1	F- ccaatgactcctatgaccccta R- cagccaagattcacggtagat	#51
UPL: Universal ProbeLibrary (Roche)			